Geochemistry and oxygen isotope composition of main-group pallasites and olivine-rich clasts in mesosiderites: Implications for the "Great Dunite Shortage" and HED-mesosiderite connection.

Richard C. Greenwood[1]; Jean-Alix Barrat[2]; Edward R. D. Scott[3]; Henning Haack[4]; Paul C. Buchanan[5]; Ian. A. Franchi[1]; Akira Yamaguchi[6]; Diane Johnson[1]; Alex W. R. Bevan[7] and Thomas H. Burbine[8]

[1]Planetary and Space Sciences, Department of Physical Sciences, The Open University, Walton Hall, Milton Keynes, MK7 6AA, United Kingdom (r.c.greenwood@open.ac.uk)
[2]CNRS UMR 6538 (Domaines Océaniques), U.B.O.-I.U.E.M., Place Nicolas Copernic, 29280 Plouzané Cedex, France.
[3]Hawaii Institute of Geophysics and Planetology, University of Hawaii at Manoa, Honolulu, HI 96822, USA.
[4]Centre for Star and Planet Formation, Natural History Museum of Denmark, Øster Voldgade 5-7, DK-1350 Copenhagen K, Denmark,
[5]Department of Chemistry and Geology, Kilgore College, 1100 Broadway, Kilgore, TX 75662, USA.
[6]National Institute of Polar Research, Tachikawa, Tokyo 190-8518, Japan and Department of Polar Science, School of Multidisciplinary Science, SOKENDAI (The Graduate University for Advanced Studies), Tachikawa, Tokyo 190-8518, Japan.
[7]Department of Earth and Planetary Sciences, Western Australian Museum, Locked Bag 49 Welshpool DC, WA 6986, Australia
[8]Astronomy Department, Mount Holyoke College, South Hadley, MA 01075, USA.

Corresponding author: Richard C. Greenwood, Email: r.c.greenwood@open.ac.uk; Tel: +44 1908 654107

Geochimica et Cosmochimica Acta (in press, july 15,2015)

Abstract- Evidence from iron meteorites indicates that a large number of differentiated planetesimals formed early in Solar System history. These bodies should have had well-developed olivine-rich mantles and consequentially such materials ought to be abundant both as asteroids and meteorites, which they are not. To investigate this "Great Dunite Shortage" we have undertaken a geochemical and oxygen isotope study of main-group pallasites and dunitic rocks from mesosiderites.

Oxygen isotope analysis of 24 main-group pallasites (103 replicates) yielded a mean $\Delta^{17}O$ value of -0.187±0.016‰ (2σ), which is fully resolved from the HED $\Delta^{17}O$ value of -0.246 ± 0.014 (2σ) obtained in our earlier study and demonstrates that both groups represent distinct populations and were derived from separate parent bodies. Our results show no evidence for $\Delta^{17}O$ bimodality within the main-group pallasites, as suggested by a number of previous studies.

Olivine-rich materials from the Vaca Muerta, Mount Padbury and Lamont mesosiderites, and from two related dunites (NWA 2968 and NWA 3329), have $\Delta^{17}O$ values within error of the mesosiderite average. This indicates that these olivine-rich materials are co-genetic with other mesosiderite clasts and are not fragments from an isotopically distinct pallasite-like impactor. Despite its extreme lithologic diversity the mesosiderite parent body was essentially homogeneous with respect to $\Delta^{17}O$, a feature best explained by an early phase of large-scale melting (magma ocean), followed by prolonged igneous differentiation.

Based on the results of magma ocean modeling studies, we infer that Mg-rich olivines in mesosiderites formed as cumulates in high-level chambers and do not represent

samples of the underlying mantle. By analogy, recently documented Mg-rich olivines in howardites may have a similar origin.

Although the Dawn mission did not detect mesosiderite-like material on Vesta, evidence linking the mesosiderites and HEDs includes: i) their nearly identical oxygen isotope compositions; ii) the presence in both of coarse-grained Mg-rich olivines; iii) both have synchronous Lu-Hf and Mn-Cr ages; iv) there are compositional similarities between the metal in both; and v) mesosiderite-like material has been identified in a howardite breccia. The source of the mesosiderites remains an outstanding question in meteorite science.

The underrepresentation of olivine-rich materials amongst both asteroids and meteorites results from a range of factors. However, evidence from pallasites and mesosiderites indicates that the most important reason for this olivine shortage lies in the early, catastrophic destruction of planetesimals in the terrestrial planet-forming region and the subsequent preferential loss of their olivine-rich mantles.

1. Introduction

A well-known and yet still poorly understood problem in both meteorite science and remote sensing studies of asteroids, is the apparent under representation of olivine-rich differentiated materials (Chapman, 1986; Bell et al., 1989; Burbine et al., 1996; Mittlefehldt et al., 1998; Scott et al., 2010). Referred to by Bell et al. (1989) as the "Great Dunite Shortage", the basis of this problem is that complete melting and subsequent differentiation of broadly chondritic asteroids (both ordinary and carbonaceous chondrites) should produce a layered body comprising a metallic core, a thick olivine-dominated mantle and a relatively thin, predominantly basaltic crust (Fig. 1)

(Righter and Drake, 1997; Ruzicka et al., 1997; Mandler and Elkins-Tanton., 2013; Toplis et al., 2013; Consolmagno et al., 2015). Evidence from iron meteorites indicates that a large number of such fully differentiated bodies formed very early in solar system history, possibly as little as 0.1 Myr after CAIs (Markowski et al., 2006; Kruijer er al., 2012, 2014). Estimates of the number of distinct differentiated asteroids from which we have core samples vary between 26 and 60 (Scott 1972; Burbine et al., 1996; Mittlefehldt et al., 1998; Haack and McCoy, 2005; Chabot and Haack, 2006; Wasson, 2013a; Benedix et al., 2014). Silicate-bearing irons, including the IAB, IIICD and IIE groups, are excluded from these estimates as they probably did not form distinct asteroidal cores. Compared to iron meteorites, silicate material that can plausibly be derived from the mantles of differentiated asteroids is significantly underrepresented in the meteorite record. Burbine et al. (2002) suggest that the differentiated and primitive achondrites and stony irons can be derived from as few as 12 parent bodies. More recently, Greenwood et al. (2012) estimated that the number of parent bodies that could have supplied meteorite samples of potential mantle origin was between 4 and 18. The upper limit of this estimate was calculated assuming that most ungrouped olivine-bearing achondrites sample distinct parent bodies, which is unlikely to be the case. Likewise, olivine-rich asteroids that are thought to be from differentiated bodies (A-types) are one of the rarest types in the main belt (Burbine et al., 1996; DeMeo et al., 2009, 2014; Burbine, 2014).

A range of explanations might account for this apparent lack of olivine–rich material: i) olivine-rich asteroids are “disguised” by space weathering (Burbine et al., 1996; Hiroi and Sasaki, 2012), ii) the meteoritic record provides a poor indication of the material present in the asteroid belt (Burbine et al., 2002) , iii) olivine-rich samples may

be preferentially destroyed by terrestrial weathering processes (Scott, 1977), iv) high viscosity and rapid heat loss in small planetesimals inhibits the formation of significant volumes of olivine cumulates (Elkins-Tanton et al., 2014), and v) differentiated asteroids accreted in the terrestrial planet-forming region and were disrupted early in Solar System history, with the mechanically weaker olivine-rich material being effectively destroyed by continuous pulverization (Burbine et al., 1996; Bottke et al., 2006; Scott et al., 2010).

If olivine-rich material was lost due to early disruption, then one class of meteorites that might be expected to preserve traces of asteroidal mantles are the mechanically strong stony-irons. Stony-irons are generally divided into two major types: the pallasites and mesosiderites (Mittlefehldt et al., 1998). Main-group pallasites, the largest of the pallasite groups, are generally considered to be impact-produced mixtures of mantle-derived olivine and core-derived molten metal (Scott, 2007; Yang et al., 2010; Tarduno et al., 2012). Alternatively, an origin by partial fusion and subsequent fractional crystallization of a chondritic source has been proposed for the main-group pallasites (Boesenberg et al., 2012). The mesosiderites are more enigmatic, consisting of metal mixed with a range of crustal and sub-crustal lithologies (Mittlefehldt et al., 1998). Although more abundant than in the howardite-eucrite-diogenite clan (HEDs), olivine-rich materials are still rare in the mesosiderites (Ruzicka et al., 1994; Kong et al., 2008), with measured modes indicating a range of between 0 and 6 vol % of total silicates (Prinz et al., 1980). Therefore, in contrast to the main-group pallasites, mesosiderites appear to be a mixture of core and crustal materials, with only scarce amounts, if any, of the intervening olivine-rich material.

As pointed out by Mittlefehldt (1980), there are compositional and textural similarities between the main-group pallasites and rare dunitic clasts found in mesosiderites. Such similarities raise the possibility that these olivine-rich clasts may not be co-genetic with the bulk of the more evolved basaltic materials found in mesosiderites. Instead, they may represent mantle materials derived from the proposed metal-rich asteroid that impacted the upper layers of the mesosiderite parent body (e.g. Hassanzadeh et al.,1990). In keeping with this possibility, it has been proposed that the olivine-rich material in mesosiderites may have been derived from an asteroidal source distinct from that of the other silicate clasts (Rubin and Mittlefehldt, 1992; Kong et al., 2008).

Despite the evidence that main-group pallasites and mesosiderites formed in distinct environments, conventional oxygen isotope studies indicated that both groups, along with the HEDs, had similar compositions and so could all be derived from a single parent body (Clayton and Mayeda, 1996). However, a subsequent higher precision study using the laser fluorination technique indicated that the main-group pallasites and mesosiderites had resolvable differences in $\Delta^{17}O$, consistent with their derivation from distinct sources (Greenwood et al., 2006). This same study also showed that the mesosiderites and HEDs have almost identical oxygen isotope compositions and, hence, could have been derived from the same parent body. However, the efficacy of laser fluorination to resolve $\Delta^{17}O$ differences between the main-group pallasites, mesosiderites and HEDs has been disputed by Ziegler and Young (2007, 2011).

In undertaking the present study our principal aims were to investigate the origin and fate of olivine-rich asteroidal materials and to re-examine the relationship between the mesosiderites, main-group pallasites and HEDs. As part of this investigation we have

undertaken further high-precision oxygen isotope analysis of main-group pallasites, which we compare to our recent results for the diogenites (Greenwood et al., 2014). We have also investigated the petrography, geochemistry and oxygen isotope composition of a coarse-grained, olivine-rich (dunite) clast from the Vaca Muerta mesosiderite, a dunite clast from the Mount Padbury mesosiderite, previously described by McCall (1966), and two dunite clasts from the Lamont mesosiderite described by Boesenberg et al. (1997). In addition, we have carried out a detailed study of the dunite NWA 2968 and dunitic and diogenitic clasts from NWA 3329.

2. Materials and analytical methods

2.1 Main-group pallasites

Analysis of main-group pallasites was undertaken on individual separated olivine grain fragments that were physically removed from hand specimen samples. Prior to loading, olivine fragments were inspected under an optical microscope to ensure that they were fresh and inclusion-free. To be certain that no weathering products were present within these olivines a subset of samples (Table 1) were leached in ethanolamine thioglycollate (EATG). This treatment has proved to be efficient at removing terrestrial weathering products, without significantly disturbing the primary oxygen isotope composition of the sample (Greenwood et al., 2012).

2.2 Mesosiderite olivine-rich clasts

A cut slice (~3 mm thickness) of a dunite clast from the Vaca Muerta mesosiderite was acquired by one of us (HH) from a dealer. The original size and shape

of the clast are unknown, but it appears to have been somewhat ovoid and at least 5 cm in diameter. A thin, 2-3 mm layer of finer-grained metal-rich matrix material is present along one edge. A polished thin section was prepared from the clast and mineral analyses were undertaken using a FEI Quanta 200 3D FIBSEM (20kV, 10nA) and Cameca SX100 microprobe (20 kV, 20 nA) at the Open University. Initial oxygen analysis of material from the edge of the Vaca Muerta dunite clast showed evidence of significant terrestrial contamination. Subsequent analyses were conducted only on fresh interior material, with some fractions being cleaned in EATG. The other mesosiderite olivine-rich clasts and dunitic lithologies analyzed in this study were leached in EATG prior to oxygen isotope analysis (Table 1).

Large single crystals of olivine and pyroxene up to 2 cm in diameter are relatively common in the Lamont mesosiderite (Boesenberg et al., 1997). Samples of two distinct olivine megacrysts, Lamont-S and Lamont-R, were obtained from the American Museum of Natural History for oxygen isotope analysis. Both samples were approximately 60 mg and were treated with EATG to remove any traces of terrestrial weathering products.

Olivine-rich enclaves showing well-developed cataclastic textures similar to the Vaca Muerta clast have been described by McCall (1966) from the Mount Padbury mesosiderite. A polished block of Mount Padbury inclusion “N” (WAM 13513.2) was prepared for microprobe analysis at the Open University. Material from inclusion “N” was treated with EATG prior to oxygen isotope analysis.

2.3 NWA 2968 and NWA 3329.

NWA 2968 was purchased in Erfoud, Morocco in 2005 and consisted of a bag of blocky, dark brown fragments (each measuring about 17-25 mm across), with a total weight of 268 g (Bunch et al. 2006). This material comprises >95 vol% Mg-rich olivine and displays textural similarities to the mesosiderite olivine-rich clasts. NWA 2968 is officially classified as an ungrouped achondrite, but Bunch et al. (2006) suggested that it showed affinities to the HEDs. A second sample of similar fragments was purchased in Er-Rachidia and is described in the Meteoritical Bulletin 91 as; "Multiple fragments of a single stone weighing 252g". This material has been classified as a diogenite and designated as NWA 3329. A number of fragments of NWA 3329 were obtained by one of us (J-A B.) and found to consist of three distinct lithologies: one that was identical to NWA 2968, a second dunitic lithology that was finer-grained than the NWA 2968-related material and a third lithology which appears to be equivalent to the original NWA 3329 diogenite. Both the original NWA 2968 material and NWA 3329 fragments show identical weathering characteristics and it seems probable to us that both are derived from the same meteorite, which is most likely a weathered mesosiderite (Barrat et al. (2010a) (see section 4.8). To avoid confusion, the coarser-grained dunite is referred to simply as NWA 2968 dunite, the finer-grained dunite as NWA 3329 dunite and the diogenite as NWA 3329 diogenite.

A sample from the original NWA 2968 material was obtained from Northern Arizona University and treated with EATG prior to oxygen isotope analysis. A more extensive study has been undertaken on the NWA 3329 dunite (ICP-MS, electron microprobe analysis, oxygen isotopes). Preliminary results of this work were given in

Barrat et al. (2010a). Fragments of the NWA 3329 dunite were treated with EATG prior to oxygen isotope analysis.

2.4 Oxygen isotopes

Oxygen isotope analysis was carried out at the Open University using an infrared laser-assisted fluorination system (Miller et al., 1999). Oxygen was released from the samples (approximate weight 2 mg) by heating in the presence of BrF_5. After fluorination, the released oxygen gas was purified by passing it through two cryogenic nitrogen traps and over a bed of heated KBr. Oxygen gas was analyzed either using a Micromass Prism III dual inlet mass spectrometer for samples run during the initial stages of this study, or later with a MAT 253 dual inlet mass spectrometer. The calibration conditions and analysis protocols were essentially identical on both instruments. Published analytical precision (2σ) for our system, based on replicate analysis of international (NBS-28 quartz, UWG-2 garnet) and internal standards, is approximately ±0.08‰ for $\delta^{17}O$; ±0.16‰ for $\delta^{18}O$; ±0.05‰ for $\Delta^{17}O$ (Miller et al., 1999). Changes to analytical procedures implemented subsequent to the system description given by Miller et al. (1999) have resulted in improvements to precision such that 39 analyses of our internal obsidian standard undertaken during six separate sessions in 2013 gave the following combined results: ±0.05‰ for $\delta^{17}O$; ±0.09‰ for $\delta^{18}O$; ±0.02‰ for $\Delta^{17}O$ (2σ). The precision (1σ) quoted for individual meteorite samples is based on replicate analyses.

Oxygen isotopic analyses are reported in standard δ notation, where $\delta^{18}O$ has been calculated as: $\delta^{18}O = [(^{18}O/^{16}O)_{sample}/(^{18}O/^{16}O)_{ref} - 1] \times 1000$ (‰) and similarly for $\delta^{17}O$ using the $^{17}O/^{16}O$ ratio, the reference being VSMOW: Vienna Standard Mean Ocean

Water. $\Delta^{17}O$, which represents the deviation from the terrestrial fractionation line, has been calculated using the linearized format of Miller (2002):

$$\Delta^{17}O = 1000\ln(1+\delta^{17}O/1000) - \lambda\, 1000\ln(1+\delta^{18}O/1000)$$

where $\lambda = 0.5247$, which was determined using 47 terrestrial whole-rock and mineral separate samples (Miller, 2002; Miller et al., 1999).

2.5 Minor and trace element analysis

Meteorite fragments were powdered using a boron carbide mortar and pestle. Two fragments of the same dunitic clast (NWA 3329, clast A1 and A2) have been analyzed. Because NWA 3329 is moderately weathered, we leached the powders in 3N HCl at 50°C for approximately half an hour. This treatment removes not only most of the secondary phases (e.g., calcite and rust), but dissolves phosphates, sulphides and part of the metal. The residues from this leaching are chiefly composed of silicates. As the interior of the Vaca Muerta clast is relatively fresh it was not leached. Minor and trace element concentrations were measured at the Institut Universitaire Europeen de la Mer (IUEM), Plouzané, by ICP-MS (inductively coupled plasma-mass spectrometry) using a Thermo Element 2 spectrometer following the procedures described by Barrat et al. (2012). Based on standard measurements and sample duplicates, concentration reproducibility is generally much better than 5 %.

3. Results

3.1 Petrography and mineralogy

Representative analyses of the main phases in both the mesosiderite dunitic clasts and related dunites are given in Table 2.

3.1.1 Dunitic clasts in Vaca Muerta and Mount Padbury mesosiderites

In thin section the Vaca Muerta clast consists predominately of relatively fresh, angular olivine grains up to 1cm in diameter (Fig. 2a). Olivines display distinct undulose extinction and broad deformation twins. A well-developed cataclastic texture is displayed throughout (Fig.2a). The interstices between the larger olivine grains are filled by finer grained, angular olivines enclosed by troilite (Fig 2b). Accessory phases in the groundmass include: Mg-bearing stanfieldite ($Mg_3Ca_3[PO_4]_4$), chromite and Cr-rich spinel, phosphoran olivine with up to 7.3 wt% P_2O_5 and a range of secondary iron oxides. Olivine compositions are in the range Mg# = 84.9 to 90.5 (where Mg# = Mg/Mg+Fe *100). However, the large olivine fragments have essentially homogeneous Mg-rich compositions (average Mg# = 88.8±2.0 (2σ)) (Table 2), except for minor zoning near some edges. The average FeO/MnO ratio of the Vaca Muerta olivines is 52.2±14.6 (2σ) (Table 2) and so somewhat higher than values generally seen in olivines from mesosiderites (e.g. Delaney et al., 1980; Mittlefehldt et al., 1998).

Mount Padbury inclusion "N" consists of fresh, coarse-grained olivine with a grain-size that may exceed 2 cm (McCall, 1966). McCall indicates that, like the Vaca Muerta clast, inclusion "N" shows a well-developed cataclastic texture in places. The polished block made for this study was limited in area (approximately 2 cm x 1 cm) and did not show any well-developed cataclastic features comparable to those seen in the

Vaca Muerta clast. However, olivine is traversed by a network of thin veinlets, 10-30 μm wide, composed mainly of iron sulphide with accessory chromite, Fe,Ni metal and phosphates (Fig. 3a,b,c). The composition of olivine in inclusion "N" is very similar to that in the Vaca Muerta clast, with Mg# in the range 86.3 to 90.8 and an average Mg# of 89.7±1.6 (2σ) (Table 2). Olivine shows only very minor normal zoning. As in the Vaca Muerta clast, the more iron-rich compositions are probably developed very close to grain edges. However, the angular olivine domains decorated by sulphides and metal (Fig 3a,b,c) are probably not original, but were produced by later brecciation. The average FeO/MnO ratio of the inclusion "N" olivines is 48.2±15.6 (2σ) and so essentially the same as the Vaca Muerta clast, with both plotting somewhat above the mesosiderite field in Fig. 4.

3.1.2 NWA 2968 and NWA 3329 dunites

Our polished section of NWA 2968 consists of the same material as described by Bunch et al. (2006). This rock is a coarse-grained dunite with shocked olivine crystals > 2 cm, which are fractured and display mosaicised domains and undulatory extinction. Small grains of orthopyroxene (< 30 μm), metal (kamacite and taenite), Ni-rich sulfides are found in the fractures (Bunch et al., 2006), as well as calcite typical of hot desert weathering. Olivine (Mg# = 91.8, FeO/MnO = 39.0±12.8 (2σ), CaO, Cr_2O_3, NiO all < 0.05 wt%) and orthopyroxene ($En_{90.8}Wo_{1.7}Fs_{7.5}$, FeO/MnO=26.7±11.2 (2σ)) are chemically homogeneous. Our results are in perfect agreement with those reported by Bunch et al. (2006).

We examined two sections of the NWA 3329 dunite, prepared from distinct clasts. Both are essentially made of olivine crystals < 5 mm, with a composition similar to NWA 2968 (Mg# = 90.9 and 91.9, FeO/MnO = 43.2±14.0 (2σ) and 43.4±16.2 (2σ)). A few grains of orthopyroxene and chromite were observed in one of the sections. In the other, a couple of grains of chromite and one crystal of stanfieldite were observed. Tiny grains of metal and sulfides occur in both sections. The olivines and orthopyroxenes in NWA 2968 and NWA 3329 dunites are among the most magnesian ever reported from HEDs or mesosiderites (Table 2, Fig. 4).

3.1.3 *NWA 3329 diogenite*

A large orthopyroxene clast weighing 15 g has been examined. A small chip has been extracted, and used for the preparation of a section. Its composition is homogeneous ($En_{64.0}Wo_{4.3}Fs_{31.7}$, FeO/MnO=29.4±4.4 (2σ)) and comparable to the most Fe-rich diogenites (i.e., the Yamato-B diogenites like Yamato 75032, Takeda and Mori, 1985). It is, however, different in composition to that previously reported for NWA 3329 (~$Wo_{2.4}Fs_{29}$, Met, Bull. 91), and suggests that the orthopyroxenes in NWA 3329 are more diverse than in a regular equilibrated diogenite.

3.2. Oxygen isotope analysis

3.2.1 Main-group pallasites

Results from the oxygen isotope analysis of 24 main-group pallasites (103 replicates) are given in Table 2 and plotted in Fig. 5. These data include our previously published results for 12 main-group pallasites (37 replicates) (Greenwood et al., 2006).

The mean $\Delta^{17}O$ value for the 24 samples is -0.187±0.016‰ (2σ) (Table 1), which is very close to the value of -0.183±0.018‰ (2σ) obtained from our previous study (Greenwood et al., 2006). The main-group pallasite results are compared in Fig. 5 with those obtained for 22 diogenites in a recent study by Greenwood et al. (2014), which gave a mean $\Delta^{17}O$ value of -0.246 ± 0.014 (2σ). The variation in the diogenites is regarded by Greenwood et al. (2014) as providing a good indication of the intrinsic variation in the HED parent body as a whole, because diogenites, being coarser-grained, more deep-seated lithologies, are less prone to impact mixing than the higher level lithologies such as basaltic eucrites and howardites. It is clear from Fig. 5 that the main-group pallasites and diogenites show no overlap in terms $\Delta^{17}O$ and appear to represent distinct populations that were derived from separate parent bodies.

3.2.2 Olivine-rich clasts in mesosiderites

Results of oxygen isotope analysis of olivine-rich clasts examined in this study are given in Table 1 and plotted in Fig. 6 in relation to our main-group pallasite data and the mesosiderite data of Greenwood et al. (2006). All of the clasts plot close to the average mesosiderite $\Delta^{17}O$ value of Greenwood et al. (2006) and are clearly resolvable from the main-group pallasites. This suggests that these clasts are co-genetic with the other silicate-bearing clasts in the mesosiderites and are not xenolithic fragments of pallasite-derived material. All of the olivine-rich mesosiderite clasts analysed in this study have much lower $\delta^{18}O$ values than the mesosiderite clasts analyzed by Greenwood et al. (2006), but display overlapping values with the main-group pallasites. This reflects the fact that, like the pallasites, the silicates in these clasts are almost exclusively olivine.

3.2.3 Dunites NWA 2968 and NWA 3329

Oxygen isotope analyses for NWA 2968 and NWA 3329 dunites are given in Table 1 and plotted in Fig. 6. Also shown on Fig. 6 is our analysis of MIL 03443 (Greenwood et al., 2014), which although it is lithologically a dunite shows more affinities to the HEDs than the mesosiderites (Beck et al., 2011). Based on their high Ni and Co contents Barrat et al. (2010a) suggested that both NWA 2968 and NWA 3329 are mesosiderite-related, rather than being members of the HED clan, as proposed by Bunch et al. (2006) in the case of NWA 2968. In keeping with this possibility both lithologies plot on the mesosiderite fractionation line of Greenwood et al. (2006) (Fig.6). However, oxygen isotopes are not able to discriminate between HEDs and mesosiderites, as both groups show almost complete compositional overlap, with the HEDs having a mean $\Delta^{17}O$ value of -0.246 ± 0.014 (2σ) (Greenwood et al., 2014) compared to -0.245 ± 0.020 (2σ) for the mesosiderites (Greenwood et al., 2006). This is illustrated by the fact that the dunite MIL 03443, which shows much closer affinities to the HEDS than either NWA 2968 or NWA 3329 (Beck et al., 2011), also plots virtually on the mesosiderite fractionation line. The possible relationship between the olivine-rich mesosiderites and HEDs is discussed further in section 4.9.

3.2.4 NWA 3329 diogenite

The orthopyroxene clast from the NWA 3329 diogenite (Table 1, Fig. 6) plots virtually on the mesosiderite fractionation line but at higher $\delta^{18}O$ values than any of the dunites.

3.3. Minor and trace element geochemistry

3.3.1 Pallasites

Olivines from pallasites characteristically display a distinct V-shaped REE pattern as typified by Springwater (Saito et al., 1998) (Fig.7). However, the REE profile for Brenham obtained by Masuda (1968) differed somewhat from that obtained by Saito et al. (1998), and as a consequence we have reanalysed Brenham as part of this study (Table 3, Fig. 7). As can be seen from Fig. 7 our new REE profile for Brenham differs significantly from that of Matsuda (1968), but displays a close resemblance to that of Springwater (Saito et al., 1998).

3.3.2 Vaca Muerta dunite clast

Selected minor and trace element analyses for the Vaca Muerta olivine-rich clast (unleached) are given in Table 3. This dunite is not Ni and Co-rich compared to other Vaca Muerta pebbles (e.g., Rubin and Mittlefehldt, 1992), but its abundances lie well on the silicates/metal mixing line with the other mesosiderites in a Ni vs. Co plot (not shown). The lithophile element abundances are low, as expected for a dunite. Such low abundances are extremely sensitive to terrestrial secondary processes. Indeed, the Sr (=0.8 µg/g) and Ba (=0.6 µg/g) abundances and the positive Ce anomaly (Ce/Ce^*=1.44) could indicate a slight degree of terrestrial contamination.

Rare Earth Element (REE) concentrations for the Vaca Muerta dunite clast (normalized to CI abundances) are plotted in Fig. 7. For comparison, the REE patterns of olivine clasts from the Dong Ujimqin Qi mesosiderite (Kong et al., 2008) are also shown

in Fig. 7. When compared to previously analyzed mesosiderite clasts, either of broadly gabbroic (Rubin and Mittlefehldt, 1992; Mittlefehldt et al., 1998; Wadhwa et al., 2003), or more ultramafic composition (Ntaflos et al., 1993; Ruzicka et al., 1999; Kong et al., 2008), the Vaca Muerta dunite has, along with NWA 3329 (see below), one of the most highly depleted REE compositions yet measured in these lithologies. In addition, the Vaca Muerta clast displays a somewhat modified V-shaped pattern compared to that seen in other mesosiderite olivine-rich clasts (Ntaflos et al., 1993; Kong et al., 2008) and some pallasites (Masuda, 1968; Saito et al., 1998; Minowa and Ebihara, 2002; this study). The origin of V-shaped REE patterns in pallasites and mesosiderites is discussed further in section 4.7.

3.3.3 NWA 3329 dunite

While the leaching treatment carried out on NWA 3329 (section 2.5) would have affected Ni and Co concentrations, their abundances are high in both fragments (Ni>1000 µg/g, Co>75 µg/g). These concentrations, especially the Ni ones are significantly higher than the values determined in MIL 03443, the sole HED-related dunite analyzed so far (Beck et al., 2011), and in diogenites (Mittlefehldt, 1994; Barrat et al., 2008; Mittlefehldt et al., 2012a). This evidence suggests that NWA 3329 is likely to be derived from mesosiderite clast material (as originally suggested by Barrat et al. (2010a)).

This dunite is poor in lithophile elements, as exemplified by the REEs (<0.3 CI). However, the REE patterns of both fragments are similar (Fig. 7), with a V-shape, and a negative Eu anomaly, a feature also displayed by olivine clasts from the Dong Ujimqin Qi mesosiderite (Kong et al. 2008) (Fig. 7).

3.3.4 NWA 3329 diogenite

The trace element abundances of the NWA 3329 clast (Table 3) are similar to some regular diogenites. Its REE pattern is identical to those of the NWA 5613 group (Barrat et al., 2010b), and characterized by light REE depletions, moderate heavy REE enrichments, and a deep negative Eu anomaly (Fig. 8).

4. Discussion

4.1 Formation models for main-group pallasites

Until recently there was general agreement that main-group pallasites were samples from the core-mantle boundary zone of a single, differentiated asteroid (e.g. Scott and Taylor, 1990; Ulff-Møller et al., 1998; Wasson and Choi, 2003). To explain the predominantly angular nature of pallasitic olivine (Scott, 1977), some form of high-energy formation event has usually been invoked, such as an impact that crushed mantle olivine into an underlying molten core (Scott and Taylor, 1990; Ulff-Møller et al., 1998; Wasson and Choi, 2003). In addition, main-group pallasites were generally considered to be derived from the same body as the IIIAB irons, which were thought to represent material from its core (Wasson and Choi, 2003). However, IIIAB irons cooled more rapidly at temperatures below about 700°C than main-group pallasites and are therefore considered to be from a distinct source (Yang et al., 2010). Yang et al. (2010) suggest that main-group pallasites are essentially impact-generated mixtures of core and mantle materials that formed as a result of a hit-and-run collision. Further evidence against a core-mantle origin for main-group pallasites has come from paleomagnetic measurements

of pallasitic olivine (Tarduno et al., 2012). These data have been used to argue that main-group pallasites formed when liquid Fe,Ni metal from the core of an impactor was injected into upper mantle material of an approximately 200 km radius protoplanet. Paleointensity measurements indicate that the protoplanet must have retained a partially liquid core for tens of millions of years after this impact event and that pallasite formation took place at relatively shallow depths in the range of 10 to 40 km (Tarduno et al., 2012). A shallow origin for some main-group pallasites has also been proposed by Davis and Olsen (1991) based on the evidence of phosphate REE patterns. In contrast to impact-related scenarios, Boesenberg et al. (2012) have proposed a model for the formation of main-group pallasites that involves fractional melting of a chondritic precursor to produce a multi-layered parent body, with subsequent fractional crystallization of residual silicate and metallic melts to produce minor phases.

4.2 Oxygen isotope evidence for the origin of main-group pallasites

In contrast to a single parent body origin (section 4.1), Ziegler and Young (2007) suggest that their oxygen isotope data for the main-group pallasites display a bimodal $\Delta^{17}O$ distribution. Ali et al. (2013, 2014) have also reported evidence in favor of a bimodal $\Delta^{17}O$ distribution, suggesting that two distinct groups are present, one with an average $\Delta^{17}O$ value of -0.213 ± 0.011 (2σ) ("Low " $\Delta^{17}O$ group) and the other -0.172 ± 0.007 (2σ) ("High" $\Delta^{17}O$ group). Seven of the ten samples used to define these groups were also analyzed in the present study. Our analyses of samples in the "Low" $\Delta^{17}O$ group (Brahin, Esquel, Fukang, Giroux) have a mean $\Delta^{17}O$ value of -0.189 ± 0.018 (2σ), compared to a value of -0.183 ± 0.018 (2σ) for our analyses of samples in the "High"

$\Delta^{17}O$ group (Brenham, Imilac, Springwater). On the basis of our data for the two groups defined by Ali et al. (2013, 2014) we find no evidence to support the possibility of a bimodal $\Delta^{17}O$ distribution within the main-group pallasites. Ali et al. (2014) suggest that their two main-group pallasite sub-groups show differences in terms of olivine content and Fo compositions. However, these data seem somewhat limited and Fukang in the "low" group plots in the "high" $\Delta^{17}O$ group with respect to Fo content.

Our results for 24 pallasites (Table 1, Fig. 5) indicate that these samples show a high level of isotopic homogeneity. In fact, the level of $\Delta^{17}O$ homogeneity shown by the main-group pallasites (±0.016‰ (2σ)) (Table 1) is comparable to that of other bodies that have experienced high levels of melting i.e. the HEDs (±0.014‰ (2σ)) (Greenwood et al., 2014), angrites (±0.014‰ (2σ)) (Greenwood et al., 2005), lunar rocks (±0.021‰ (2σ)) (Hallis et al., 2010), SNCs (±0.026‰ (2σ)) (Franchi et al., 1999). In contrast, primitive achondrite groups, which experienced much lower degrees of melting, have much more heterogeneous $\Delta^{17}O$ values i.e. ±0.36‰ (2σ) in the case of the acapulcoites and lodranites (Greenwood et al., 2012). This evidence suggests that main-group pallasites are derived from a single source that was extremely homogeneous with respect to $\Delta^{17}O$.

Our data for the main-group pallasites are clearly resolvable from the HED suite (Fig. 5) in terms of their $\Delta^{17}O$ values, indicating that these groups are not derived from a single parent body (Greenwood et al., 2006). Distinct average $\Delta^{17}O$ values for the HEDs (-0.238 ± 0.062 (2σ)) and main-group pallasites (-0.204 ± 0.062 (2σ)) were also obtained by Ziegler and Young (2007). However, the level of precision achieved in their study resulted in significant overlap between the two groups, which led the authors to suggest

that main-group pallasites and HEDs could not be separated on the basis of their oxygen isotope compositions. A further study by Ziegler and Young (2011), which investigated the main-group pallasite Esquel, did not alter this overall conclusion, although their average $\Delta^{17}O$ for the main-group pallasites was shifted slightly to -0.199 ± 0.058 (2σ). A recent study of 3 HEDs and 6 main-group pallasites (Jabeen et al., 2013) obtained distinct average $\Delta^{17}O$ values for the two groups of -0.272 ± 0.012 (2σ) and -0.213 ± 0.011 (2σ), respectively. On the basis of these results, and in agreement with Greenwood et al. (2006), Jabeen et al. (2013) concluded that the HEDs and main-group pallasites are fully distinguishable in terms of their $\Delta^{17}O$ values and as a consequence are samples from distinct parent bodies.

It has recently been suggested by Wasson (2013a) that main-group pallasites, IIIAB irons and HEDs all originate from the same parent body. However, the fact that HEDs and main-group pallasites show no overlap in terms of their $\Delta^{17}O$ compositions (Fig. 4) rules out this possibility (Greenwood et al., 2014).

4.3 Models for the origin of mesosiderites

Mesosiderites are essentially composed of basaltic, gabbroic and orthopyroxene-rich clasts, as well as minor dunitic clasts, enclosed by Fe,Ni metal and troilite (Mittlefehldt et al., 1998; Scott et al., 2001). Unlike pallasites, olivine-rich "dunitic" material is relatively uncommon in mesosiderites (Mittlefehldt et al., 1998). Thus, mesosiderites can be viewed as a core-crust mix in contrast to the core-mantle mix seen in pallasites. Mixing core and crustal materials to form the mesosiderites without also sampling significant amounts of the intervening olivine-rich mantle necessarily requires

complex formation conditions (Mittlefehldt et al., 1998). This scenario is further complicated by the two-stage thermal history of mesosiderites, which cooled rapidly at high temperatures and much more slowly at lower temperatures. Thus, Delaney et al. (1981) estimated cooling rates of between 1 and 100ºC per year at temperatures in the range 900 - 1150 ºC based on Fe-Mg profiles in pyroxenes. Ruzicka et al. (1994) estimated cooling rates at peak metamorphic temperatures (850-1100 ºC) of ≥0.1 ºC per year based on plagioclase overgrowth textures in the Morristown and Emery mesosiderites. In comparison, cooling rates during kamacite growth at ~500 ºC were 0.2-0.5 ºC/Ma (Hopfe and Goldstein, 2001).

Although a wide range of models have been put forward to explain the formation conditions of mesosiderites (Hewins, 1983), it is now generally accepted that to account for the extensive metamorphism and partial melting experienced by the silicate material during silicate-metal mixing, the metal must have been almost entirely molten (Hassanzadeh et al., 1990; Rubin and Mittlefehldt, 1993; Scott et al., 2001). Recent disagreements concerning the mode of formation of the mesosiderites have been concerned with whether the metal and silicate-rich components were derived from the same or two distinct parent bodies and the extent of parent body disruption that was involved i.e. local or total. Thus, Hassanzadeh et al. (1990) suggested that the mesosiderites formed when the molten core of an asteroid impacted the surface layers of a second differentiated asteroid. In contrast, Scott et al. (2001) proposed that the metal and silicate components in mesosiderites were both predominantly derived from the same 200-400 km diameter differentiated asteroid, which had a molten core prior to its total disruption by a 50-150 km diameter projectile.

4.4 Oxygen isotope evidence for the origin of mesosiderite olivine-rich clasts

Since the olivine-rich clasts plot on the extension of the mesosiderite fractionation line (Fig. 6) they are probably co-genetic with the other silicate-bearing material in the mesosiderites. The suggestion by Rubin and Mittlefehldt (1992) and Kong et al. (2008) that olivine in mesosiderites may be derived from a distinct parent body to that of the other silicate clasts is not supported by our oxygen isotope data. Although the concept of a magma ocean has been criticized when applied to relatively small asteroidal bodies (Wasson, 2013b), the homogeneity of the mesosiderites with respect to $\Delta^{17}O$ is best explained by an early phase of extensive melting. This is analogous to the proposed mechanism for oxygen isotopic homogenization in the angrites and HEDs (Greenwood et al., 2005, 2014). Protracted differentiation, after early, large-scale melting, would have led to the lithological diversity seen in the mesosiderites (McCall 1966; Floran 1978; Mittlefehldt 1980; Mittlefehldt et al. 1998) and result in mass dependent oxygen isotope fraction, as shown by the spread in $\delta^{18}O$ values displayed by the various mesosiderite clast types (Greenwood et al. 2006 and this study).

4.5 Regolith processes on the mesosiderite parent body

Unlike main-group pallasites, olivine-rich rocks in the mesosiderites are intimately intermixed with basalts, gabbros and orthopyroxenites (Mittlefehldt et al. 1998). As discussed in the previous section, oxygen isotope evidence indicates that all these diverse clast types are derived from the same parent body. However, an important question concerns the nature of the process by which these materials were brought

together. One possibility, in the case of the olivine-rich clasts, is that the impact event that mixed metal and silicate to produce the mesosiderites also dredged up deep-seated olivine-rich material and mixed this into a pre-existing breccia. However, this seems less likely than the alternative possibility that the olivine-rich material had already been mixed with other clast types prior to the metal-silicate mixing event.

Olivine-rich material is not an abundant component in mesosiderites, representing between 0 and 6 vol% of their silicate portion (Prinz et al. 1980). As Mittlefehldt (1980) points out, the silicate portion of mesosiderites appears to represent an asteroidal regolith breccia consisting of an intimate mixture of various clast types, predominantly gabbros and orthopyroxenites, but also including olivine crystal fragments and dunite clasts. In addition to the examples described here, olivine-rich clasts have been identified in a significant number of other mesosiderites. Mittlefehldt (1980) characterized cm-sized single crystal fragments of olivine in Mincy and Pinnaroo with compositions of $Fo_{90.1}$ and Fo_{92} respectively and, hence, compositionally similar to the olivines in this study. Kong et al. (2008) presented a study of a suite of olivine-rich clasts from the Dong Ujimqin Qi mesosiderite and Ruzicka et al. (1994) documented corona textures in Morristown and Emery formed by reaction between olivine mineral clasts and the enclosing matrix assemblage. Nehru et al., (1980) undertook an extensive survey of 20 mesosiderites and demonstrated that olivine fragments, as relatively large clasts measuring 1mm to 7mm, were present in all but 2 of the samples studied. The fact that olivine clasts are so ubiquitous in mesosiderites and that they appear to be well mixed with the other more common clast types argues against a single event for their emplacement. Rather, it suggests that these clasts are an indigenous component of the mesosiderite silicate

fraction and were probably present prior to the metal silicate mixing event. Olivine clasts in mesosiderites show evidence of significant brecciation (Fig. 2a,b) leading to the development of a cataclastic texture (McCall, 1966). However, the timing of this deformation, relative to the metal-silicate mixing event, is unclear.

As discussed in section 4.3, the mesosiderite silicate fraction was mixed with metal during an impact event that most likely involved a projectile that was essentially a molten metal core, with very little, if any, associated mantle material (Hassanzadeh et al. (1990). The fact that the core was molten was originally proposed by Hassanzadeh et al. (1990) based on the evidence that mesosiderite metal is essentially homogeneous and therefore could not have fractionally crystallized. In addition, many mesosiderite basaltic and gabbroic clasts show evidence of remelting after metal-silicate mixing (Rubin and Mittlefehldt, 1992; Mittlefehldt et al., 1998). This impact event presumably did not involve total parent body disruption otherwise the amount of olivine-rich material would have been much greater than is actually observed. However, this evidence is not entirely conclusive as we have no way of knowing whether the mesosiderites are entirely representative of the original breccias present on their parent body. Following their formation, the resulting metal-silicate breccias must have been deeply buried within the parent body to account for the extremely slow metallographic cooling rates measured in mesosiderites (section 4.3).

4.6 Olivine-rich clasts in mesosiderites – mantle or cumulate origin?

Oxygen isotope data (section 4.4) does not support the possibility that Mg-rich olivines in mesosiderites were derived from the metal-rich impactor responsible for the

metal-silicate mixing event. In view of this constraint, what are the likely sources for these olivine-rich clasts? There would appear to be two possible end-member origins: either they represent high-level cumulates of Mg-rich melts or, alternatively, they are samples of the mesosiderite mantle. Distinguishing between these possibilities is not straightforward. Even for a relatively large asteroid, such as the mesosiderite parent body, the cumulates that formed its mantle will be compositionally and textural very similar to the higher-level cumulates of Mg-rich melts.

In the case of the dunite MIL 03443, Beck et al. (2011) argue that it represents a high-level cumulate related to the diogenites. In view of its Fe-rich olivine composition (Mg#=74), diogenite-like FeO/MnO ratio (42.7) (Fig. 4) and REE abundances this would seem to be a convincing interpretation. In comparison, the significantly more magnesian composition of olivine in the Vaca Muerta and Mount Padbury dunites and related rocks (NWA 2968, NWA 3329) (average Mg# = 88.3 to 91.8) (Table 2) (Fig.4) precludes an origin as cumulates from relatively evolved liquids, equivalent to those that produced the regular diogenites. It is therefore possible that these olivine-rich rocks are samples from the mantle of the mesosiderite parent body. However, magnesian-rich diogenites are known i.e. MET 00425 (Barrat et al., 2008; Mittlefehldt et al., 2012a) and NWA 1461 (Bunch et al., 2007) and so an origin for the clasts as cumulates of more Mg-rich diogenite-like magmas seems an equally viable option.

Since the mesosiderite parent body is estimated to have been of similar size and bulk composition to that of the HEDs (Haack et al., 2003), one way of assessing the likely origin of the dunitic clasts and related rocks is to compare their compositions to the

predictions of models for the progressive crystallization of a Vesta-like parent body (Righter and Drake, 1997; Ruzicka et al. ,1997; Mandler and Elkins-Tanton, 2013).

Ruzicka et al. (1997) have presented a magma ocean model for Vesta involving fractional crystallization of a chondrite-like starting composition. Their model predicts a thick basal cumulate layer of olivine with a composition of $Fo_{93-80.}$ These values bracket those found in the mesosiderite clasts and also the NWA 2968 and NWA 3329 dunites and so, if the model of Ruzicka et al. (1997) is realistic, this might suggest that these lithologies could represent materials derived from the mantle of their parent body. However, if this is the case, an outstanding problem is how such materials were removed from the mantle and then incorporated into a regolith without totally disrupting the parent body.

The fractional crystallization model of Ruzicka et al. (1997) has been criticized by both Righter and Drake (1997) and Mandler and Elkins-Tanton (2013) on the basis that the liquids produced by this process are too Fe-rich compared to natural eucrites. Instead of a single stage fractional crystallization model, both Righter and Drake (1997) and Mandler and Elkins-Tanton (2013) have proposed two stage models involving an initial phase of equilibrium crystallization of a whole asteroid magma ocean, followed by extraction of the residual melt, which then undergoes fractional crystallization in high level magma chambers to produce the observed variation seen in the HED meteorites.

The schemes of Righter and Drake (1997) and Mandler and Elkins-Tanton (2013) differ mainly in the stage at which the residual melt is extracted from the crystallizing magma ocean. Righter and Drake (1997) suggest that this took place after 80% crystallization, whereas Mandler and Elkins-Tanton (2013) suggest that it was after 60 to 70%

crystallization. As a consequence, in the model of Righter and Drake (1997) these expelled residual liquids are more evolved than those of Mandler and Elkins-Tanton (2013) and so produce high-level cumulates that contain more Fe-rich olivine. The calculations of Righter and Drake (1997) suggest that olivine crystallizing from such a residual liquid would have a value of Mg# =74, which is significantly more Fe-rich than the olivines found in the mesosiderite dunites.

In their recent study, Mandler and Elkins-Tanton (2013) suggest that, while the Righter and Drake (1997) model is more successful than that of Ruzicka et al. (1997), it still does not reproduce satisfactorily the observed variation in the HED meteorites. The more primitive residual liquid modelled by Mandler and Elkins-Tanton (2013) produces initial dunites with an olivine composition close to Fo_{90}. This is well within the range observed in the mesosiderite dunite clasts. It is important to note that because both the models of Righter and Drake (1997) and Mandler and Elkins-Tanton (2013) are based on an initial stage of equilibrium crystallization of a magma ocean, the final olivines present in the mantle would be more Fe-rich than those found in the mesosiderites and related rocks. One implication of both models, provided they are realistic, is that they exclude the possibility that the mesosiderite Mg-rich clasts are of mantle origin. Based on a comparison with the predictions of the Mandler and Elkins-Tanton model, the most likely origin of the Mg-rich mesosiderite olivines is that they represent the initial cumulates formed by fractional crystallization within high-level magma chambers.

However, both fractional and equilibrium crystallization are likely to have been highly inefficient processes in the setting of an evolving early-formed planetesimal. Elkins-Tanton et al. (2014) point out that fractional crystallization within a magma ocean

on Vesta is extremely unlikely. This is because a magma ocean on a small asteroidal body, without an atmosphere, would be cooling rapidly due to a high heat flux from its outer surface. This would be particularly so if the solid crust was continually foundering and being re-assimilated. The magma ocean would also have had a high effective viscosity, contain a crystal fraction throughout its depth and so crystals would have to have been relatively large (several to 10cm) before they would start to settle (Elkins-Tanton et al., 2014). On the other hand, efficient equilibrium crystallization, as envisaged in the initial stages of the models of Righter and Drake (1997) and Mandler and Elkins-Tanton (2013), is also unlikely. As noted, early-formed asteroids would have been cooling rapidly and would also have been subject to frequent impact events. Such a continuous bombardment would have been inevitable in the early Solar System and result in the repeated removal of the body's insulating crust and so increased the global cooling rate (Gupta and Sahijpal, 2010).

In reality, differentiation of Vesta-like bodies was probably complex and messy. Residual liquids extracted from the magma ocean crystal mush were unlikely to be of uniform composition and so would have produced a variety of cumulate products when they underwent crystallization within crustal magma chambers. In fact even two stage magma ocean models for Vesta (Mandler and Elkins-Tanton, 2013) may not be able to explain all of the compositional diversity displayed by the HEDs and in particular the range of parental liquids that gave rise to the diogenites (Barrat and Yamaguchi (2014). However, even given these caveats, the olivine compositions calculated for the initial high-level cumulates by Mandler and Elkins-Tanton (2013) are remarkably close to those observed in the mesosiderite dunites. On the basis of this evidence it would seem more

likely that the Mg-rich olivine clasts in mesosiderites represent material derived from high-level disrupted plutons, rather than being samples from the deep mantle.

4.7 Rare earth element patterns in main-group pallasites and mesosiderite olivine-rich clasts and related dunites.

Olivine from both main-group pallasites and olivine-rich clasts in mesosiderites characteristically displays a V-shaped REE pattern (Fig. 7) (Masuda, 1968; Saito et al., 1998; Kong et al., 2008; Minowa and Ebihara, 2002; this study). A range of explanations have been advanced to explain the origin of these patterns. On the basis of experimental results, Saito et al. (1998) interpreted them in terms of olivine crystallization at near liquidus temperatures of around 1450°C. However, the partition coefficients derived by Saito et al. (1998) differ from those obtained in other studies, i.e. Beattie (1994) and Bédard (2005), which indicate that values increase progressively from La to Lu. To explain the V-shaped REE patterns seen in pallasites, Minowa and Ebihara (2002) suggested that it may reflect terrestrial contamination. They modelled the light REE enriched component as being equivalent to typical crustal rocks on Earth, which they combined with pallasitic olivine displaying a progressively light REE depleted pattern. Minowa and Ebihara (2002) suggest that a 0.001% addition of such a terrestrial contaminant could explain the Brenham profile obtained by Masuda (1969). However, olivine-rich clasts in the Dong Ujimqin Qi mesosiderite fall invariably display V-shaped REE patterns (Fig. 7) (Kong et al., 2008) indicating that terrestrial contamination is unlikely to be a general explanation for these profiles. Phosphates in pallasites show highly variable REE patterns and concentrations (Davis and Olsen, 1991; Hsu, 2003).

Thus, whitlockite and stanfieldite in the Springwater main-group pallasite are highly enriched in REEs compared to CIs and show light REE enriched patterns (Davis and Olsen, 1991). Thus, the characteristic V-shaped pattern observed in pallasites and olivine-rich clasts in mesosiderites may reflect the influence of both olivine as the dominant phase and phosphate as a highly enriched REE-bearing accessory phase.

While the patterns obtained by Kong et al. (2008) for olivine clasts from the Dong Ujimqin Qi mesosiderite are similar to those obtained by us for the Vaca Muerta and NWA 3329 dunites, the Dong Ujimqin Qi examples are generally more highly enriched in REEs. Kong et al. (2008) suggest that the relatively high REE concentrations that they measured in Dong Uimqin Qi indicate that olivine must have formed from a melt that was highly enriched in REEs, particularly light REEs. On the basis of this evidence they suggest that the olivine clasts may be from a source that is distinct from that of the other silicates found in mesosiderites. As discussed in section 4.3, oxygen isotope evidence does not support a distinct origin for the olivine-rich clasts compared to the other silicate-rich materials in mesosiderites. One possible explanation for the high REE concentrations measured by Kong et al. (2008) is that at least some of the clasts they studied were enriched in a phosphate component. The material selected by Kong et al. (2008) does not seem to have been leached prior to analysis and was only crushed to a relatively coarse grain-size (1mm) prior to hand-picking under a binocular microscope.

4.8 NWA 2968 and NWA 3329 – Are they related to the mesosiderites or HEDs or both?

Olivine-rich “dunitic” rocks have now been identified that appear to have affinities both to the mesosiderites (NWA 2968 and NWA 3329) (Barrat et al., 2010a)

and HEDs (MIL 03443) (Beck et al. 2011). In terms of their $\Delta^{17}O$ values these meteorites are indistinguishable (Fig. 6). However, both dunitic fractions of NWA 3329 have significantly higher Ni values (1872 and 1005 ppm) (table 3) than MIL 03443 (61 ppm) (Beck et al., 2011). On a plot of Mg# vs. FeO/MnO (Fig. 4) MIL 03443 falls well within the diogenite field, whereas NWA 2968 and NWA 3329 dunites plot close to the Vaca Muerta and Mount Padbury clasts with respect to the Mg# of their olivines, but have somewhat lower FeO/MnO ratios. As suggested by Barrat et al. (2010a), this evidence indicates that the NWA 2968 and NWA 3329 dunites are more closely related to the mesosiderites than to the HEDs. Further, the extremely magnesian nature of the olivines in NWA 2968 and NWA 3329 suggests that, like the Vaca Muerta and Mount Padbury olivine-rich clasts, these rocks are either samples from the upper mantle of the mesosiderite parent body, or alternatively cumulates from highly magnesian melts.

As noted in section 2.3, besides containing two distinct dunitic fractions NWA 3329 also contains diogenitic material. The REE profile for the NWA 3329 diogenite (Fig. 8) is light REE depleted with a marked Eu anomaly and shows a striking resemblance to the patterns seen in the NWA 5613 group of diogenites (Barrat et al., 2010b). On the basis of their similar weathering characteristics it is likely that both the diogenitic and dunitic fractions of NWA 3329 represent clast material from a single mesosiderite meteorite. The fact that the NWA 3329 diogenitic material is a virtual clone in terms of its REE pattern for the NWA 5613 diogenite group is further evidence of the close affinity between mesosiderites and HEDs (Mittlefehldt et al. 1998). The nature of this relationship is examined in further detail below.

4.9 The relationship between the mesosiderites and HEDs – Are they both from a common source?

It has long been recognized that the silicate-rich fraction in mesosiderites shows bulk compositional and mineralogical similarities to the major lithological components of the HEDs (Rubin and Mittlefehldt, 1993; Mittlefehldt et al., 1998; Haack et al., 2003; Bunch et al. 2014). However, distinct geochemical differences also exist between these two broadly basaltic suites, in particular in terms of their REE patterns (Prinz et al., 1980; Rubin and Mittlefehldt, 1992, 1993; Mittlefehldt et al., 1998). One major problem in interpreting the origin of these differences is the extent to which they are primary in nature, or alternatively reflect the extensive post-formational reheating experienced by the mesosiderites during the metal-silicate mixing event (Floran et al., 1978; Mittlefehldt et al., 1998). Additional evidence that is cited against a common origin for the HEDs and mesosiderites comes from the manganese-chromium dating study of Wadhwa et al. (2003), which found that a global Mn/Cr fractionation event took place ~2 Ma later on the mesosiderite parent body than that of the HEDs. In contrast, a more recent study by Trinquier et al. (2008) found that the Mn-Cr isochrones for mesosiderites and HEDs were indistinguishable and so concluded that both could be derived from the same parent body. Evidence cited in favor of a common source for the HEDs and mesosiderites includes their virtually identical oxygen isotope compositions (Greenwood et al., 2005, 2006, 2014, this study), the presence of mesosiderite-like material in howardites (Rosing and Haack, 2004), similarities between metal in some HEDs and mesosiderites (Yamaguchi et al., 2006) and synchronous Lu-Hf ages for the cumulate eucrites and mesosiderites (Haack et al., 2003).

Haack et al. (1996, 2003) presented evidence indicating that the HED and mesosiderite parent bodies were probably of a similar size. Spectral evidence suggests that the asteroid 4 Vesta (~ 520 km diameter) is the source of the HED meteorites (Binzel and Xu, 1993; Drake, 2006; McSween et al. 2011). Haack et al. (2003) suggest that if the mesosiderites formed on a distinct asteroid of similar size to the HEDs, then it should be relatively easy to locate, provided it has remained intact. One possible candidate is the Maria asteroid family as they provide a reasonable spectral match to the mesosiderites (Fieber-Beyer et al., 2011). However, this possibility is not universally accepted as Vernazza et al. (2014) relate the Maria family to the ordinary chondrites. While the possibility that the HEDs and mesosiderites are both from the same source remains controversial (Mittlefehldt et al. 2012b; Bunch et al., 2014; Scott et al., 2014) measurements by Dawn's GRaND instrument (Gamma-Ray and Neutron Detector) demonstrate that mesosiderites are not a major component of Vesta's regolith (Prettyman et al., 2012; Peplowski et al., 2013). This should not be surprising given the evidence that mesosiderites cooled extremely slowly at depth (section 4.3).

A further piece of evidence potentially linking the two groups is the presence of highly magnesian olivines in both howardites (Delaney et al., 1980; Lunning et al., 2014, 2015; Hahn et al., 2015) and mesosiderites (sections 4.5 and 4.6). The olivine grains described by Lunning et al. (2014, 2015) are said to be unzoned, monomineralic clasts, with compositions (Mg# = 80 to 92 and molar Fe/Mn of 37 to 45) that overlap the mesosiderite Mg-rich olivines (Fig. 9). Lunning et al. (2015) have undertaken oxygen isotopic analysis of these Mg-rich olivine grains by secondary ion mass-spectrometry. The results obtained demonstrate that these olivines are not derived from an exogenic

chondritic source and instead indicate that they originated from the HED parent body itself. Recently, Mg-rich harzburgitic clasts have been described from a number of paired Antarctic howardites, which have Fe/Mn ratios for both olivine and pyroxene that are also consistent with an HED source (Hahn et al., 2015).

While the majority of olivines in howardites appear to be derived from diogenitic material (Fig. 9), the more magnesian grains may come from a distinct source, which Lunning et al. (2014, 2015) and Hahn et al. (2015) suggest may be the HED parent body mantle. Olivines in mesosiderites define a broad compositional field with a slight trend of increasing FeO/MnO with increasing Mg# (Fig. 4, Fig. 9). In comparison, the diogenites display more limited variation with respect to Mg# and generally higher FeO/MnO ratios, although there is some overlap with the mesosiderites (Fig. 4, Fig. 9). The simplest interpretation of such differences is that the HEDs and mesosiderites represent material from two distinct parent bodies (Delaney et al. 1980). However, the lower FeO/MnO ratio of mesosiderites compared to howardites at low Mg# values may reflect reduction of olivine associated with metal/silicate mixing. Note that at the high Mg# values relevant to this study there is significant overlap between the mesosiderite and howardite fields in Fig. 9.

A potentially significant objection to a mantle origin for high magnesian olivines in howardites (Delaney et al. 1980; Lunning et al. 2014, 2015; Hahn et al., 2015) and mesosiderites (if from the same source as the HEDs), comes from Dawn remote sensing data indicating that olivine-rich rocks are not exposed within the deep, composite southern basin on Vesta (e.g., Ammannito et al., 2013a; Clenet et al., 2014a). The presence of such olivine-rich units had been predicted by pre-Dawn observations (Binzel

et al., 1997; Gaffey, 1997), and given that material in the basins may have come from depths greater than 50 km (Jutzi et al. 2013), would theoretically be of mantle origin. The lack of olivine-rich units in the southern basin indicates that the crust-mantle boundary on Vesta is deep (Clenet et al., 2014b). Olivine has recently been detected on Vesta in near-surface materials (Ammannito et al., 2013b; Ruesch et al., 2014), but is interpreted as either reflecting the presence of small ultramafic bodies within the crust (Ruesch et al. 2014), or alternatively is due to exogenic impact-related materials (Nathues et al., 2014). If these olivine-rich rocks are indigenous to Vesta they may be equivalent to the diogenite-related dunites such as MIL 03443 (Beck et al. 2011) and so would support models for the origin of diogenites by emplacement of discrete plutons at high crustal levels (Barrat et al., 2008, 2010b; Yamaguchi et al., 2011).

Laboratory tests indicate that the predicted mantle composition of Vesta (60-80 % olivine according to Mandler and Elkins-Tanton, 2013) should be clearly resolvable from diogenite-like material using the Dawn's Visible InfraRed spectrometer (VIR) (Beck et al., 2013). Clenet et al. (2014b) have recently suggested that Dawn's failure to detect mantle materials on Vesta indicates that "its bulk chemical composition deviates from a chondritic composition". Consolmagno et al. (2015) are in agreement with this conclusion and also point to the chemical trends exhibited by the HEDs (Na depletion, FeO abundance, trace element distributions), as evidence that either Vesta formed from a non-chondritic source, or experienced a post-formational hit-and- run style collision that significantly modified its global composition. If this is correct it would invalidate any conclusions drawn from current magma ocean models which are based on broadly chondritic starting compositions. In conclusion, the lack of exposed mantle rocks on

Vesta would seem to favour a high-level cumulate origin for the magnesian olivines in howardites and, by inference, possibly also those in mesosiderites.

4.10 Early-formed asteroids – so where is all the olivine?

Planetary formation in the inner Solar System is widely viewed as having taken place in a series of relatively distinct stages (Chambers, 2004; Weidenschilling and Cuzzi, 2006). Initially dust grains in the nebula clumped to produce kilometer-sized or larger bodies, termed planetesimals. Interactions between planetesimals caused them to combine to form a few tens of Moon-to-Mars-size planetary embryos within approximately 0.1 to 1 million years of Solar System formation. Finally, in the following 100 million years or so, planets were formed by collisions between these embryos (Chambers, 2004). As a result of heating, principally due to the decay of short-lived radionuclides, most notably ^{26}Al ($t_{½}$ = 0.7Myr), early-formed planetesimals would have melted and undergone differentiation into metallic cores and silicate-rich mantles and crusts (Gosh and McSween, 1998; Hevey and Sanders, 2006). Finding evidence for this earlier planetesimal stage of Solar System evolution is problematic, as the vast majority of such bodies were lost during the collisional disruption that ultimately led to the formation of the planets, including Earth. Bottke et al. (2006) suggest that early-formed differentiated planetesimals were more likely to have accreted in the terrestrial planet-forming region than the main belt. They modeled this process and showed that most of the early-formed 20 to 100 km planetesimals in the 0.5 to 1.5 AU region would have undergone disruption within a few million years of formation. Some material from these

disrupted bodies would have been scattered into the main belt, with a small fraction eventually being delivered to Earth as meteorites (Bottke et al., 2006).

If it is assumed that these melted planetesimals were of broadly chondritic composition we can estimate the relative proportions of meteorite samples that we should have in our collections from the core, mantle and crust of these differentiated bodies. Toplis et al. (2013) provide analysis of the predicted characteristics of fully differentiated Vesta-sized bodies for a range of chondritic starting compositions. In terms of percentage by mass, mantle material should predominate, ranging from approximately 61 to 82% of these bodies, depending on their starting compositions. Core material varies from 6 to 30% and crustal material from 5 to 19%. All things being equal, which they clearly are not (see below), the analysis of Toplis et al. (2013) indicates that we might expect to have at least three or four times as many mantle samples as core samples in our collections. In reality, as outlined in the introduction, iron meteorites that can plausibly be derived from the cores of differentiated asteroids are significantly more abundant than mantle-derived samples (Mittlefehldt et al., 1998; Scott et al., 2010), and the same appears to be true for asteroids (Chapman, 1986; Bell et al., 1989; Burbine et al., 1996). Bell et al. (1989) referred to this as the "Great Dunite Shortage", but in fact this is something of a misnomer. Strictly speaking a dunite is an ultramafic rock containing greater than 90% modal olivine (Streckeisen, 1974). Only planetesimals with carbonaceous chondrite bulk starting compositions are likely to have mantles with >90% olivine (Toplis et al., 2013), whereas bodies derived from ordinary chondrite precursors will have harzburgitic mantles, with between about 55% to 80% olivine (Toplis et al., 2013; Mandler and Elkins-Tanton, 2013). In the case of enstatite chondrite bulk compositions, olivine is

subordinate to pyroxene (Toplis et al. 2013). If the present day preponderance of ordinary chondrites is a reliable indicator of the bulk composition of these early-formed planetesimals, then the "Great Dunite Shortage" is really the "Great Harzburgite Shortage"!

A wide range of possible reasons for the apparent underrepresentation of olivine-rich, mantle-derived materials have been advanced, however, these can be divided into two broad categories: 1) those that potentially influence the present asteroid and meteorite populations, and 2) those that affected their primordial distributions. Explanations that fall into the first category include: i) the influence of space-weathering, which may "disguise" olivine-rich asteroids (Burbine et al., 1996; Hiroi and Sasaki, 2012); ii) meteorites do not provide a systematic sampling of the asteroid belt, but instead are dominated by material from a few young asteroid families (Burbine et al., 2002; Bottke, 2014) , iii) terrestrial weathering processes may preferentially destroy olivine-rich samples (Scott, 1977); iv) iron meteorites (and stony-irons) are much more robust than silicate-rich meteorites and so survive longer in space as small objects, as shown by their significantly higher cosmic ray exposure ages (Mittlefehldt et al., 1998; Eugster, 2003); and v) the Yarkovsky effect perturbs the orbits of rocks with lower thermal conductivities, including olivine-rich materials, on a shorter timescale than higher conductivity objects such as iron meteorite (Bottke et al., 2006). Dunites and other olivine-rich rocks will therefore drift into resonances on a shorter time-scale than the irons (Bottke et al., 2006). Explanations that relate to the primordial distribution of olivine-rich materials include: i) early-formed differentiated planetesimals may have had non-chondritic or enstatite chondrite-like bulk compositions and hence did not crystallize

significant olivine in their mantles (Consolmagno et al., 2015); ii) high viscosity and rapid heat loss in small planetesimals inhibits the formation of significant volumes of olivine cumulates (Elkins-Tanton et al., 2014); iii) differentiated asteroids accreted in the terrestrial planet-forming region and were disrupted early in Solar System history, with the mechanically weaker olivine-rich material being effectively destroyed by continuous pulverization (Burbine et al., 1996; Bottke et al., 2006; Scott et al., 2010); iv) early-formed planetesimals had extremely low alkali abundances (e.g. HEDs and angrites), with lack of Na promoting the formation of anorthite ($CaAl_2Si_2O_8$) compared to albite ($NaAlSi_3O_8$), and as a consequence of the lower silica to alumina ratio of anorthite, orthopyroxene crystallization was promoted at the expense of olivine (Consolmagno et al., 2015).

The above list is far from comprehensive, but serves to demonstrate that the missing olivine problem is probably multifactorial and has as much to do with the preferential preservation of metal-rich meteorites (including stony-irons) as it is about the preferential loss of olivine.

What insight into this problem is provided by the mesosiderites and pallasites? Apart from the fact that they are both composed of roughly equal amounts of silicate and metal (± sulphide), pallasites and mesosiderites are very different meteorite types. However, the feature they have in common is that catastrophic impact processes appear to have played a central role in their formation. In the case of the mesosiderites, as discussed in section 4.3, there is a general acceptance that their formation involved the impact of a denuded, essentially molten, iron core from a differentiated asteroid into the surface layers of a second differentiated body. One might have expected that this molten

core would have retained some of the overlying mantle material and that this might be represented by the dunite clasts that are the subject of this study. But the oxygen isotope and compositional evidence presented here do not support this possibility. Instead, it would seem that the mantle of the mesosiderite iron impactor was completely stripped prior to impact. A similar event appears to be central to the formation of the main-group pallasites. While *in situ* models have been advanced recently (Boesenberg et al., 2012) (see section 4.1), paleointensity measurements suggest that main-group pallasite formation involved the impact of a denuded molten metal core into the upper mantle of second differentiated body (Tarduno et al., 2012). If this model is realistic, and as was discussed above for the mesosiderites, it might be expected that some adhering mantle olivine was retained by the postulated main-group pallasite iron impactor. However, reports of a bimodal oxygen isotope signature in the main-group pallasites are not supported by the results of this study (section 4.2) and we find no evidence for silicate material that could be derived from the metal-rich impactor. The various pallasite types, of which the main-group is the largest, appear to be derived from up to seven distinct parent bodies (Scott, 2007). If similar impact processes to those advanced for the main-group operated on all these bodies it suggests that core denudation and subsequent catastrophic impact were widespread processes in the early Solar System. It is also worth noting that recently Consolmagno et al. (2015) advanced the possibility of catastrophic mantle stripping to account for the lack of exposed olivine on Vesta.

The evidence from mesosiderites and pallasites suggests that hit-and-run style collisions between bodies were probably commonplace in the early Solar System (Asphaug et al., 2006). Simulations suggest that during such encounters the smaller of the

two colliding bodies can be torn apart, resulting in relatively efficient separation of mantle and core material (Asphaug et al., 2006). Modelling by Asphaug and Reufer (2014) indicates that during accretion of the inner planets hit and run style collisions would have been commonplace, with planetesimals often experiencing multiple encounters leading to efficient mantle stripping. As outlined above, core material (iron meteorites) has a significantly higher survivability than mantle (olivine-rich) silicates. Thus, mantle material removed from its core would have had a relatively poor chance of long-term survival and so become rapidly lost from the asteroid and meteorite records (Gaffey, 1985; Chapman, 1986; Burbine et al., 1996).

However, we do have olivine-rich mantle samples in our collections in the form of ureilites and so a "battered-to-bits" model alone (Burbine et al., 1996) cannot account for the overall paucity of such olivine-rich samples. Ureilites are generally regarded as representing mantle-derived debris from a now disrupted, differentiated, carbon-rich asteroid (e.g. Downes et al., 2008; Barrat et al., 2015). The ureilite parent body (UPB) appears to have been fully differentiated, as indicated by newly identified crustal material (Bischoff et al., 2014) and evidence that it underwent core formation (e.g. Warren et al., 2006; Barrat et el., 2015). The UPB experienced catastrophic destruction (Downes et al. 2008), so why was its mantle not eliminated from the meteorite and asteroidal records? One possibility is that the UPB, based on its carbon-rich bulk composition, was unlikely to have accreted in the terrestrial planet-forming region, but further out, where collisional interactions were less intense (Bottke et al. (2006),

From the above discussion, it is clear that the missing mantle problem is certainly the result of many factors. However, the evidence from the pallasites and mesosiderites

seems to suggest that the single most important reason for the paucity of olivine in asteroids and meteorites lies in the early, catastrophic destruction of differentiated planetesimals formed within the terrestrial planet region and the subsequent preferential loss of their olivine-rich mantles (Burbine et al., 1996; Bottke et al., 2006; Yang et al., 2010). In contrast, the cores of these bodies were more robust and as a result iron and stony-iron meteorites provide a more enduring legacy from this initial stage of planetary evolution.

5. Conclusions

The principal conclusions of this study are as follows:

1. Our oxygen isotope data for main-group pallasites indicate that they form a single homogeneous population, consistent with their derivation from a single common parent body. We see no evidence for $\Delta^{17}O$ bimodality within the main-group pallasites, as suggested by other recent studies.

2. Oxygen isotope evidence is consistent with the olivine-rich clasts in mesosiderites being co-genetic with the other silicate-rich clasts and therefore they do not represent xenolithic fragments derived from a pallasite-like impactor. Earlier proposals that olivine in mesosiderites may be derived from a different parent body to that of the other silicates is not supported by our oxygen isotope data. The mesosiderite parent body was both lithologically diverse and essentially homogeneous with respect to $\Delta^{17}O$. The homogeneity of the mesosiderites with

respect to $\Delta^{17}O$ is best explained by an early phase of extensive melting, analogous to the proposed mechanism for oxygen isotopic homogenization in the angrites and HEDs.

3. Despite the lack of evidence from the Dawn mission for the presence of mesosiderites on the surface of 4 Vesta there remain multiple lines of evidence linking them with the HEDs. This evidence includes: i) their nearly identical oxygen isotope compositions, ii) the presence in both of texturally and compositionally similar magnesian, coarse-grained olivines, iii) synchronous Lu-Hf and Mn-Cr ages, iv) compositional similarities between metal in some HEDs and mesosiderites and, v) the presence of mesosiderite-like material in howardites. Set against this evidence is the fact that mesosiderite clasts show greater compositional diversity, particularly in their trace elements, than analogous HED lithologies. The source of the mesosiderites, whether from Vesta or another differentiated asteroid, remains an important open question in meteorite science.

4. Based on a comparison with the results of studies modeling the progressive crystallization of molten chondritic asteroids, we infer that olivine-rich clasts in mesosiderites were derived from disrupted high-level cumulates from magnesian magmas rather than being samples of a mantle formed by progressive crystallization of a magma ocean. Recently documented Mg-rich olivines in howardites may similarly be of crustal rather than mantle origin.

5. The underrepresentation of olivine-rich, mantle-derived materials amongst both asteroids and meteorites, the so-called "Great Dunite Shortage", probably results from a range of factors. However, evidence from pallasites and mesosiderites suggests that the single most important reason for the paucity of olivine in asteroids and meteorites lies in the early, catastrophic destruction of planetesimals within the terrestrial planet-forming region and the subsequent, preferential loss of their olivine-rich mantles.

6. Acknowledgements

Oxygen isotope studies at the Open University are funded through a Science and Technology Funding Council Consolidated Grant to the Department of Physical Sciences. Jenny Gibson is thanked for all her help and assistance with oxygen isotope analysis work at the Open University. We would like to thank the Associate Editor Anders Meibom for his efficient handling of the manuscript. We are very grateful to Duck Mittlefehldt and Joe Boesenberg for their helpful, constructive and thought-provoking reviews. We are grateful to Don Stimpson for providing samples of olivine from Brenham for ICP-MS work and Fabien Kuntz for providing material from NWA 3329.

References

Ali A., Jabeen I., Banerjee N. R., Tait K. T., Hyde B. C., Nicklin I. and Gregory D. (2013) Potential for bimodality in main group pallasites: An oxygen isotope perspective. 75th *Meteoritical Society Meeting* #5243 (abstr.)

Ali A., Jabeen I., Banerjee N. R., Osinski G. R., Tait K. T., Hyde B. C., Nicklin I., Ganderon T. and Gregory D. (2014) Oxygen isotope variations in main group pallasites and HEDs. *Lunar Planet. Sci. XLV*. Lunar Planet Inst. #2390 (abstr.).

Ammannito E. et al. (2013a) Vestan lithologies mapped by the visual and infrared spectrometer on Dawn. *Meteorit. Planet. Sci.* **48,** 2185-2198.

Ammannito E. et al. (2013b) Olivine in an unexpected location on Vesta**'s surface.** ***Nature*** **504**, doi:10.1038/nature12665.

Asphaug E. and Reufer A. (2014) Mercury and other iron-rich planetary bodies as relics of inefficient accretion. *Nature Geosci.* **7**, 564-568.

Asphaug, E., Agnor C. B. and Williams, Q. (2006) Hit-and-run planetary collisions. *Nature* **439**, 155-159.

Barrat J-A. and Yamaguchi A. (2014) Comment on "The origin of eucrites, diogenites, and olivine diogenites: Magma ocean crystallization and shallow magma processes on vesta" by B.E. Mandler and L.T. Elkins-Tanton. *Meteorit. Planet. Sci.* **49**, 468-472.

Barrat J-A., Beck P., Bohn M., Cotton J., Gillet P., Greenwood R.C. and Franchi I. A. (2006) Petrology and geochemistry of the fine-grained unbrecciated diogenite Northwest Africa 4215. *Meteorit. Planet. Sci.* **41**, 1045-1057.

Barrat J-A., Yamaguchi A., Greenwood R. C., Benoit M., Cotten J., Bohn M. and Franchi I.A. (2008) Geochemistry of diogenites: Still more diversity in their parental melts. *Meteorit. Planet. Sci.* **43**, 1759-1775.

Barrat J-A., Greenwood R. C., Yamaguchi A., Bohn M., Bollinger C., Franchi I. A. (2010a) Northwest Africa 2968/3329: Dunitic and diogenitic pebbles from the same mesosiderite fall? *Meteorit. Planet. Sci.* **45**, #5304 (abstr).

Barrat J-A., Yamaguchi A., Zanda B., Bollinger C. and Bohn M. (2010b) Relative chronology of crust formation on asteroid Vesta: Insights from the geochemistry of diogenites. *Geochim. Cosmochim. Acta* **74**, 6218-6231.

Barrat J-A., Zanda B., Moynier F., Bollinger C., Liorzou C. and Bayon G. (2012) Geochemistry of CI chondrites: Major and trace elements and Cu and Zn isotopes. *Geochim. Cosmochim. Acta* **83**, 79-92.

Barrat J-A., Rouxel O., Wang K., Moynier F., Yamaguchi A., Bischoff A. and Langlade J. (2015) Early stages of core segregation recorded by Fe isotopes in an asteroidal mantle. *Earth planet Sci. Lett.*, **419**, 93-100.

Beattie P. (1994). Systematics and energetics of trace-element partitioning between olivine and silicate melts: implications for the nature of mineral/melt partitioning. *Chem. Geol.* **117**, 57– 71.

Beck A.W. and McSween H.Y. (2010). Diogenites as polymict breccias composed of orthopyroxenite and harzburgite. *Meteorit. Planet. Sci*. **45**, 850-872.

Beck A. W., Mittlefehldt D., McSween H. Y, Rumble D., Lee C. T. and Bodnar R. (2011) MIL 03443, a dunite from asteroid 4 Vesta Evidence for its classification and cumulate origin. *Meteorit. Planet. Sci*. **46**, 1133-1151.

Beck A.W., McCoy T.J., Sunshine J.M., Viviano C.E., Corrigan C.M., Hiroi T. and Mayne R.G. (2013) Challenges in detecting olivine on the surface of 4 Vesta. *Meteorit. Planet. Sci*. **46**, doi: 10.1111/maps. 12160.

Bédard J.H. (2005) Partitioning coefficients between olivine and silicate melts. *Lithos* **83**, 394-419.

Benedix G.K., Haack H., and McCoy T.J. (2014) Iron and stony-iron meteorites. In *Meteorites and Cosmochemical Processes* (A.M. Davis, ed.) Vol. 1, *Treatise on Geochemistry, Second edition*, pp. 267-285, Elsevier, Oxford.

Bell J.F., Davis D.R., Hartmann W.K. and Gaffey M.J. (1989). Asteroids: The big Picture. In *Asteroids II* ed. by Binzel R.P., Gehrels T., Matthews M.S. University of Arizona Press, Tucson, pp.921-945.

Binzel, R. P. and Xu, S. (1993) Chips off of asteroid 4 Vesta – Evidence for the parent body of basaltic achondrite meteorites. *Science* **260**, 186-191.

Binzel R.P., Gaffey M.J., Thomas P.C., Zellner B.H., Storrs A.D. and Wells E.N. (1997) Geologic mapping of Vesta from 1994 Hubble Space Telescope images. *Icarus* **128**, 95-103.

Bischoff A., Horstman M., Barrat J-A., Chaussidon M., Pack A., Herwartz D., Ward D., Vollmer C. and Decker S. (2014) Trachyandesitic volcanism in the early solar system. Natl. Acad. Sci. USA 111(35), 12689-12692.

Boesenberg J. S., Delaney J. S. And Prinz M. (1997). Magnesian megacrysts and matrix in the mesosiderite Lamont. *Lunar Planet. Sci. XXVIII*. Lunar Planet. Inst., Houston #1491 (abstr.).

Boesenberg J. S., Delaney J. S. And Hewins R. W. (2012) A petrological and chemical reexamination of Main Group pallasite formation. *Geochim. Cosmochim. Acta*. **89**, 134-158.

Bottke W.F. (2014) On the origin and evolution of Vesta and the V-type asteroids. Conference item: Vesta in the light of Dawn: First exploration of a protoplanet in the asteroid belt. Abstract #2024.

Bottke W.F., Durda D.D., Nesvornýa D., Jedicke R., Morbidelli A.,Vokrouhlický D. and Levison H.F. (2005) Linking the collisional history of the main asteroid belt to its dynamical excitation and depletion. *Icarus* **179**, 63-94.

Bottke, W.F., Nesvorný, D., Grimm, R.E., Morbidelli, A. and O'Brien, D.P. (2006) Iron meteorites as remnants of planetesimals formed in the terrestrial planet region. *Nature* **439**, 821-824.

Bunch T.E., Wiitke J.H., Rumble III D., Irving A.J. and Reed B. (2006) Northwest Africa 2968: A dunite from 4 Vesta. *Meteorit. Planet. Sci.* **41** supplement, abstract #5252 (abstr.).

Bunch T. E., Irving A. J., Wittke J. H., Kuehner S. M. and Rumble D. (2007) Distinctive magnesian, protogranular, and polymict diogenites from Northwest Africa, Oman, and United ArabEmirates. *Meteorit. Planet. Sci*. **42**, A27.

Bunch T.E., Irving A.J., Schultz P.H., WittKe J.H., Kuehner S.M., Goldstein J.I. and Sipiera P.P. (2014) Assessment of the mesosiderite-diogenite connection and an impact model for the genesis of mesosiderites. *Lunar Planet. Sci. XLV*. Lunar Planet. Inst., Houston #2554 (abstr.).

Burbine T. H. (2014) Asteroids. In *Meteorites and Cosmochemical Processes* (A. M. Davis, ed.) Vol. 2, Treatise on Geochemistry, Second edition, pp. 365-414, Elsevier, Oxford.

Burbine, T.H., Meibom, A. And Binzel, R.P. (1996) Mantle material in the main belt: Battered to bits? *Meteoritics* **31**, 607-620.

Burbine T.H., McCoy T.J., Meibom A., Gladman B. and Keil K. (2002) Meteoritic Parent Bodies: Their Number and Identification. In *Asteroids III*, W. F. Bottke Jr., A. Cellino, P. Paolicchi, and R. P. Binzel (eds), University of Arizona Press, Tucson, pp.653-667

Chabot N.L. and Haack H. (2006) Evolution of Asteroidal Cores. In *Meteorites and the Early Solar System II*, D. S. Lauretta and H. Y. McSween Jr. (eds.), University of Arizona Press, Tucson, 943 pp.747-771.

Chambers J.E. (2004) Planetary accretion in the inner Solar System, *Earth Planet. Sci. Lett.* **223**, 241-252.

Chapman C.R. (1986) Implications of the inferred compositions of the asteroids for their collisional evolution. *Mem. Soc. Astron. Italiana* **57**, 103-114.

Clayton R. N. and Mayeda T. K. (1996) Oxygen isotope studies of achondrites. *Geochim. Cosmochim. Acta.* **60**, 1999-2017.

Clenet H., Jutzi M., Barrat J-A. and Gillet P. (2014a) Adapted modified gaussian model : No detection of olivine in regions predicted to be mantle-rich from models of planet-scale collisions. Conference item: Vesta in the light of Dawn: First exploration of a protoplanet in the asteroid belt. Abstract #2013.

Clenet H., Jutzi M., Barrat J-A., Asphaug E.I., Benz W. and Gillet P. (2014b) A deep crust-mantle boundary in the asteroid 4Vesta. *Nature* **511**, 303-306.

Consolmagno G.J., Golabek G.J., Turrini D., Jutzi M., Sirono S., Svetsov V. and Tsiganis K. (2015) Is Vesta an intact and pristine protoplanet? Icarus 254, 190-201.

Davis A.M. and Olsen E.J. (1991) Phosphates in pallasite meteorites as probes of mantle processes in small planetary bodies. *Nature* **353**, 637-640.

Delaney J.S., Nehru C.E. and Prinz M. (1980) Olivine clasts from mesosiderites and howardites: Clues to the nature of achondritic parent bodies. *Proc. Lunar Planet. Sci. Conf.* **11th**, 1073-1087.

Delaney, J. S., Nehru, C. E., Prinz, M. And Harlow, G. E. (1981) Metamorphism in mesosiderites. *Proc. Lunar Planet. Sci.* **12B,** 1315-1342.

DeMeo F.E., Binzel R.P., Silvan S.M., and Bus S.J. (2009) An extension of the Bus asteroidal taxonomy into the near-infrared. *Icarus* **202**, 160-180.

DeMeo F.E., Carry B., Binzel R.P., Moskovitz N., Polishook D. and Burt B.J. (2014) The distribution of mantle material among main-belt asteroids. American Astronomical Society Meeting #224, #321.09.

Downes H., Mittlefehldt D., Kita N.T. and Valley J.W. (2008) Evidence from polymict ureilite meteorites for a disrupted and re-accreted single ureilite parent asteroid gardened by several distinct impactors. *Geochim. Cosmochim. Acta* **72**, 4825-4844.

Drake, M. J. (2006) The Vesta-HED connection. Workshop on Early Planetary Differentiation. LPI Contrib. No. 1335, 28-29.

Elkins-Tanton L.T., Mandler B.E. and Fu R.R. (2014) Placing Vesta in the range of planetesimal differentiation models. Conference item: Vesta in the light of Dawn: First exploration of a protoplanet in the asteroid belt. Abstract #2034.

Eugster O. (2003) Cosmic ray exposure ages of meteorites and lunar rocks and their significance. *Chem. Erde* **63**, 3-30.

Fieber-Beyer S.K., Gaffey M.J., Kelley M.S., Reddy V., Reynolds C.H. and Hicks A. (2011) The Maria asteroid family: Genetic relationships and a plausible source of mesosiderites near the 3:1 Kirkwood gap. *Icarus* **213**, 524-537.

Franchi I.A., Wright I.P., Sexton A.S. and Pillinger C.T. (1999) The oxygen-isotopic composition of Earth and Mars. *Meteorit. Planet. Sci.* **34**, 657-661.

Floran, R. J. (1978) Silicate petrography, classification, and origin of the mesosiderites: Review and new observations. Proc. Lunar Planet. Sci. Conf. 9th, 1053-1081.

Gaffey M.J. (1985) A paradigm sor the S-Asteroids: Implications for the evolutionary history of the inner belt and the search for ordinary chondrite parent bodies *Lunar Planet. Sci. XVI*. Lunar Planet Inst. pp. 258-259 (abstr.).

Gaffey M.J. (1997) Surface lithological hererogeneity of asteroid 4 Vesta. *Icarus* **127**, 130-157.

Ghosh A. and McSween H.Y. 1998. A thermal model for the differentiation of asteroid 4 Vesta, based on radiogenic heating. *Icarus* **134**, 187-206.

Greenwood R.C., Franchi I.A., Jambon A. and Buchanan P.C. (2005) Wisespread magma oceans on asteroidal bodies in the early solar system. *Nature* **435**, 916-918.

Greenwood, R.C., Franchi, I.A., Jambon, A., Barrat, J.A. and Burbine, T.H. (2006) Oxygen isotope variation in stony-iron meteorites. *Science* **313**, 1763-1765.

Greenwood R.C., Franchi I.A., Gibson J.M. and Benedix G.K. (2012) Oxygen isotope variation in primitive achondrites: The influence of primordial, asteroidal and terrestrial processes. *Geochim. Cosmochim. Acta* **94**, 146-163.

Greenwood R. C., Barrat J-A., Yamaguchi A., Franchi I. A., Scott E. R. D., Bottke W. F. and Gibson J. M. (2014) The oxygen isotope composition of diogenites: Evidence for early global melting on a single, compositionally diverse, HED parent body. *Earth Planet. Sci. Lett.* **390**, 165-174.

Gupta G. and Sahijpal S. (2010) Differentiation of Vesta and the parent bodies of other achondrites. *Journal of Geophysical Research* 115:E08001.

Haack, H. and McCoy, T.J. (2005) Iron and stony-iron meteorites. In Meteorites, Comets and Planets: Treatise on Geochemistry, Volune 1. Ed. By A.M. Davis. Elsevier, The Netherlands 325-345.

Haack H., Scott E.R.D. and Rasmussen K.L. (1996) Thermal and shock history of mesosiderites and their large parent asteroid. *Geochim. Cosmochim. Acta* **60**, 2609-2619.

Haack, H., Bizzarro, M., Baker, J. A. and Rosing, M. (2003) Early thermal evolution and sizes of the HED and mesosiderite parent bodies; New constraints from Lu-Hf chronology. *Lunar Planet. Sci. XXXIV*. Lunar Planet. Inst., Houston #1317 (abstr.).

Hahn T.M., McSween H.Y. and Taylor L.A. (2015) Vesta's missing mantle: Evidence from new harzburgite components in howardites. *Lunar Planet. Sci. 46*, Lunar Planet. Inst., Houston #1964 (abstr.).

Hallis L.J., Anand M., Greenwood R.C., Miller M.F., Franchi I.A. and Russell S.S. (2010) The oxygen isotope composition, petrology and geochemistry of mare basalts:

Evidence for large-scale compositional variation in the lunar mantle. *Geochim. Cosmochim. Acta* **74**, 6885-6899.

Hassanzadeh, J., Rubin, A. E. and Wasson, J. T. (1990) Composition of large metal nodules in mesosiderites: Links to iron meteorite group IIIAB and the origin of mesosiderite subgroups. *Geochim. Cosmochim. Acta* **54**, 3197-3208.

Hevey P.J. and Sanders I.S. (2006) A model for planetesimal meltdown by 26Al and its implications for meteorite parent bodies. *Meteorit. Planet. Sci*. **41**, 95-106.

Hewins, R. H. (1983) Impact versus intenal origins for mesosiderites. Proc. 14th Lunar Planet. Sci. Conf., *J. Geophys. Res*. **88**, B257-B266.

Hiroi T. and Sasaki S. (2012) Asteroidal space weathering: compositional dependency and influence on taxonomy. Asteroids comets and meteors, conference proceedings. abstract #6109

Hopfe, W. D. and Goldstein, J. I. (2001) The metallographic cooling rate method revised: Application to iron meteorites and mesosiderites. *Meteorit. Planet. Sci*. **36**, 135-154.

Hsu, W., 2003. Minor element zoning and trace element geochemistry of pallasites. *Meteorit. Planet. Sci.* **38**, 1217-1241.

Irving A.J., Kuehner S.M., Rumble D., Hupe A.C. and Hupe G.M. (2003) Olivine diogenite NWA 1459: plumbing the depths of 4 Vesta. *Lunar Planet. Sci. XXXIV*. Lunar Planet. Inst., Houston #1502(abstr.).

Jabeen I., Banerjee N. R., Ali A., Tait K. T., Hyde B. C., Nickin I. and Gregory D. (2013) Triple oxygen isotope variations in main group pallasites and HEDs. Meteoritics and Planetary Science Supplement. Abstract #5305.

Jutzi M., Asphaug E., Gillet P., Barrat J-A. and Benz W. (2013) The structure of the asteroid 4Vesta as revealed by models of planet-scale collisions. *Nature* **494**, 207-210.

Kong, P., Su, W., Li, X., Spettel, B., Palme, H. and Tao, K. (2008) Geochemistry and origin of metal, olivine clasts, and matrix in the Dong Ujimqin Qi mesosiderite. *Meteorit. Planet. Sci.* **43**, 451-460.

Kruijer T.S., Sprung P., Kleine T., Leya I., Burkhardt C. and Weiler R. (2012) Hf-W chronometry of core formation in planetesimals inferred from weakly irradiated iron meteorites. *Geochim. Cosmochim. Acta* **99**, 287-304.

Kruijer T.S., Touboul M., Fischer-Gödde M., Bermingham K.R., Walker R.J. and Kleine T. (2014) Protracted core formation and rapid accretion of protoplanets. *Science* **344**, 1150-1154.

Lorenz C., Nazarov M., Kurat G., and Brandstaetter F. (2000) High-magnesium lithologies and dry fluid metasomatism in the Budulan mesosiderite. *Lunar Planet. Sci. XXXI*. Lunar Planet. Inst., Houston #1315 (abstr.).

Lunning N.G., McSween H.Y., Tenner T.J. and Kita N.T. (2014) Olivine from the mantle of 4 Vesta identified in howardites. *Lunar Planet. Sci. XLV*. Lunar Planet. Inst., Houston #1921 (abstr.).

Lunning N.G., McSween H.Y., Tenner T.J., Kita N.T. and Bodnar R.J. (2015) Olivine and pyroxene from the mantle of asteroid 4 Vesta. *Earth Planet. Sci. Lett*. **418**, 126-135.

Mandler B.E. and Elkins-Tanton L.T. (2013) The origin of eucrites, diogenites, and olivine diogenites: Magma ocean crystallization and shallow magma chamber processes on Vesta. *Meteorit. Planet. Sci*. **48**, 2333-2349. Doi:10.1111/maps12135.

Markowski, A., Quitté, G., Halliday, A.N. and Kleine, T. (2006) Tungsten isotopic compositions of iron meteorites: Chronological constraints vs. cosmogenic effects. *Earth Planet. Sci. Lett.* **242**, 1-15.

Masuda A. (1968) Lanthanide concentrations in the olivine phase of the Brenham pallasite. *Earth Planet. Sci. Lett.* **5**, 59-62.

McCall, G. J. H. (1966) The petrology of the Mount Padbury mesosiderite and its achondrite enclaves. *Min. Mag*. **35**, 1029-1060.

McSween Jr. H.J., Mittlefehldt D.W., Beck A.W., Mayne R.G. and McCoy T.J. (2011) HED meteorites and their relationship to the geology of Vesta and the Dawn mission. *Space Sci. Rev*. **163**, 141-174.

Miller, M. F. (2002) Isotopic fractionation and the quantification of ^{17}O anomalies in the oxygen three-isotope system: an appraisal and geochemical significance. *Geochim. Cosmochim. Acta* **66**, 1881-1889.

Miller, M.F., Franchi, I.F., Sexton, A.S. and Pillinger, C.T. (1999) High precision $\delta^{17}O$ Isotope Measurements of Oxygen from Silicates and Other oxides: Methods and Applications. *Rapid Commun. Mass Spectrom.* **13**, 1211-1217.

Minowa, H. and Ebihara, M. (2002) Rare Earth Elements in pallasite olivines. *Lunar Planet. Sci. XXXIII*. Lunar Planet. Inst., Houston #1386 (abstr.).

Mittlefehldt, D. W. (1980) The composition of mesosiderite olivine clasts and implications for the origin of pallasites. *Earth Planet. Sci. Lett.* **51**, 29-40.

Mittlefehldt D.W. (1994) The genesis of diogenites and HED parent body petrogenesis. *Geochim. Cosmochim. Acta* **58**, 1537-1552.

Mittlefehldt D.W. (2000) Petrology and geochemistry of the Elephant Moraine A79002 diogenite. *Meteorit. Planet. Sci.* **35**, 901-912.

Mittlefehldt, D. W., McCoy, T. J., Goodrich, C. A. and Kracher A. (1998) Non-chondritic meteorites from asteroidal bodies. In *Planetary Materials* (ed. J. J. Papike). *Reviews in Mineralogy*. **36**, 4-1 – 4-195, Mineralogical Society of America.

Mittlefehldt D.W., Beck A.W., Lee C-T., McSween H.Y. and Buchanan P.C. (2012a) Compositional constraints on the genesis of diogenites. *Meteorit. Planet. Sci.* **47**, 72-98.

Mittlefehldt D.W., Prettyman T.H., Reedy R.C., Beck A.W., Blewett D.T., Gaffey M.J., Lawrence D.J., McSween H.Y. and Toplis M.J. (2012b) Do mesosiderites reside on 4 Vesta? An assessment based on Dawn GRaND data. *Lunar Planet. Sci. XLIII*. Lunar Planet. Inst., Houston #1655 (abstr.).

Nathues N et al. (2014(Exogenic olivine on Vesta from Dawn Framing Camera colour data. *Icarus* DOI:10.1016/j.icarus.2014.09.045.

Nehru C.E., Zucker S.M., Harlow G.E. and Prinz M. (1980) Olivines and olivine coronas in mesosiderites. *Geochim. Cosmochim. Acta* **44**, 1103-1118.

Ntaflos, Th., Kurat, G., Koeberl, C. and Brandstätter, F., (1993). Mincy dunite F6241B: The missing ultramafic component from mesosiderites. *Meteoritics* **28**, 414 (abstract).

Peplowski P.N., Lawrence D.J., Prettyman T.H., Yamashita N., Bazell D., Feldman W.C., LeCorre L., McCoy T.J., Reddy V., Reedy R.C., Russel C.T. and Toplis M.J. (2013) Compositional variability on the surface of 4 Vesta revealed through GRaND measurements of high-energy gamma rays. *Meteorit. Planet. Sci.* **48**, 2252-2270.

Prettyman T.H. et al. (2012) Elemental mapping by Dawn reveals exogenic H in Vesta's regolith. *Science* **338**, 242-246. doi:10.1126/science.1225354.

Prinz, M., Nehru, C.E., Delaney, J.S., Harlow, G.E. and Bedell, R.L. (1980) Modal studies of mesosiderites and related achondrites, including the new mesosederite ALHA 77219. Proc. 11th Lunar Planet. Sci. Conf., 1055-1071.

Righter, K. and Drake, M.J. (1997) A magma ocean on Vesta: Core formation and petrogenesis of eucrites and diogenites. *Meteorit. Planet. Sci.* **32**, 929-944.

Rosing, M. T. and Haack, H. (2004) The first mesosiderite-like clast in a howardite. *Lunar Planet. Sci. XXXV*. Lunar Planet. Inst., Houston #1487 (abstr.).

Rubin, A. E. and Mittlefehldt D. W. (1992) Classification of mafic clasts from mesosiderites: Implications for endogenous igneous processes. *Geochim. Cosmochim. Acta.* **56**, 827-840.

Rubin, A. E. and Mittlefehldt D. W. (1993) Evolutionary history of the mesosiderite asteroid: A chronological and petrological synthesis. *Icarus* **101**, 201-212.

Ruesch O. et al. (2014) Distribution of the near-IR spectral signature of olivine on Vesta with VIR/Dawn data: The ultramafic side of Vesta's surface. *Lunar Planet. Sci. XLV*. Lunar Planet. Inst., Houston #1715 (abstr.).

Ruzicka, A., Boynton, W.V. and Ganguly, J. (1994) Olivine coronas, metamorphism, and the thermal history of the Morristown and Emery mesosiderites. *Geochim. Cosmochim. Acta.* **58**, 2725-2741.

Ruzicka, A., Snyder, G.A. and Taylor, L.A. (1997) Vesta as the HED Parent Body: Implications for the Size of a Core and for Large-Scale Differentiation. *Meteorit. Planet. Sci.* **32**, 825-840.

Ruzicka, A., Boesenberg, J. S., Snyder, G. A., Prinz, M. and Taylor, L. A. (1999) Rare-Earth-Element abundances of clasts and matrix in the Lamont mesosiderite: complex spatial variations. *Lunar Planet. Sci. XXX*. Lunar Planet. Inst., Houston #1516 (abstr.).

Sack R.O., Azeredo W.J. and Lipschutz M.E. (1991) Olivine diogenites: The mantle of the eucrite parent body. *Geochim. Cosmochim. Acta.* **55**, 1111-1120.
.

Saito T., Shimizu H. and Masuda A. (1998). Experimental study of major and trace element partitioning among olivine, metallic phase and silicate melt using chondrite as starting material: Implications for V-shaped REE patterns of the pallasite meteorites. *Geochem. J*., **32**, 159-182.

Schearer C.K., Burger P. and Papike J.J. (2010). Petrogenetic relationships between diogenites and olivine diogenites: Implications for magmatism on the HED parent body. Geochim. Cosmochim. Acta 74, 4865-4880.

Scott E. R. D., 1972. Chemical fractionation in iron meteorites and its interpretation. *Geochim. Cosmochim. Acta* **36**, 1205-1236.

Scott E.R.D. (1977) Formation of olivine-metal textures in pallasite meteorites. *Geochim. Cosmochim. Acta* **41**, 693-710.

Scott E. R. D. (2007). Impact origins for pallasites. *Lunar Planet. Sci. XXXVIII*. Lunar Planet. Inst., Houston #2284 (abstr.).

Scott E.R.D. and Taylor G. 1990. Origins of pallasites at the core-mantle boundaries of asteroids. *Lunar Planet. Sci. XXI.* Lunar Planet. Inst., Houston 1119-1120 (abstr.).

Scott, E. R. D., Haack, H. and Love, S. G. (2001) Formation of mesosiderites by fragmentation and reaccretion of a large differentiated asteroid. *Meteorit. Planet. Sci.* **36**, 869-881.

Scott E. R. D., Goldstein J. I., Yang J., Asphaug E. and Bottke W. F. (2010) Iron and stony-iron meteorites and the missing mantle meteorites and asteroids. *Meteorit. Planet. Sci.* (supplement) abstract #5015 (abstr.).

Scott E.R.D., Bottke W.F., Marchi S. and Delaney J.S. (2014) How did the mesosiderites form and do they come from Vesta or a Vesta-like body. *Lunar Planet. Sci. XLV*. Lunar Planet. Inst., Houston #2260 (abstr.).

Streckeisen A. (1974) Classification and nomenclature of plutonic rocks. *Geologische Rundschau* **63**, 773-785.

Takeda H. and Mori H. (1985) The diogenite-eucrite links and the crystallization history of a crust of their parent body. Proc. Lunar Planet. Sci. Conf. 15th Part 2: *J. Geophys Res.* 90:C636-C648.

Tarduno J.A., Cottrell R.D., Nimmo F., Hopkins J., Voronov J., Erickson A., Blackman E., Scott E.R.D. and McKinley R. (2012) Evidence for a dynamo in the main group pallasite parent body. *Science* **338**, 939-942.

Terribilini D., Eugster O., Mittlefehldt D.W., Diamond L.W., Vogt S. and Wang D. (2000) Mineralogical and chemical composition and cosmic-ray exposure history of two mesosiderites and two iron meteorites. *Meteorit. Planet. Sci.* **35**, 617-628.

Toplis M.J., Mizzon H., Monnereau M., Forni O., McSween H.Y., McCoy T.J., Mittlefehldt D.W., Prettyman T.H., De Sanctis M.C., Raymond C.A. and Russell C.T. (2013) Chondritic models of 4 Vesta: Implications for geochemical and geophysical properties. *Meteorit. Planet. Sci.* **48**, 2300-2315.

Trinquier A., Birck J-L., Allegre C.J., Göpel C. and Ulfbeck D. (2008) ^{53}Mn-^{53}Cr systematic of the early solar system revisited. *Geochim. Cosmochim Acta* **72**, 5146-5163.

Ulff-Møller F., Choi B-G., Rubin A.E., Tran J. and Wasson J.T. (1998) Paucity of sulphide in a large slab of Esquel: New perspectives on pallasite formation. Meteorit. Planet. Sci. **33**, 221-227.

Vernazza P., Zanda B., Binzel R.P., Hiroi T., DeMeo F.E., Birlan M., Hewins R., Ricci L., Barge. and Lockhart. (2014) Multiple and fast: The accretion of ordinary chondrite parent bodies. *Ap. J.* **791**, 120.

Wadhwa, M., Shukolyukov A., Davis, A. M., Lugmair, G. W., and Mittlefehldt, D. W., (2003) Differentiation history of the mesosiderite parent body: Constraints from trace elements and manganese-chromium isotope systematics in Vaca Muerta silicate clasts. *Geochim. Cosmochim. Acta.* **67**, 5047-5069.

Warren P.H., Ulff-Moller F., Huber H. and Kallemeyn G.W. 2006. Siderophile geochemistry of ureilite: a record of early stages of planetesimal core formation. *Geochim. Cosmochim. Acta.* **70**, 2104-2126.

Wasson J. T. (2013a) Vesta and extensively melted asteroids: why HED meteorites are probably not from Vesta. *Earth Planet. Sci. Lett.* **381**, 138-146.

Wasson J.T. (2013b) No magma ocean on Vesta (or elsewhere in the asteroid belt): volatile loss from HEDs. *Lunar Planet. Sci. XLIV*. Lunar Planet. Inst., Houston #2836 (abstr.).

Wasson J.T. and Choi B-G. (2003) Main-group pallasites: Chemical composition, relationship to IIIAB irons, and origin. *Geochim. Cosmochim. Acta.* **67**, 3079-3096.

Weidenschilling S.J. and Cuzzi J.N. (2006) Accretion dynamics and timescales: Relation to chondrites. In Meteorites and the Early Solar System II. Ed by D.S. Lauretta and H.Y. McSween Jr. University of Arizona Press, Tucson 943 pp 473-485.

Yamaguchi, A., Okamoto, C. and Ebihara, M., (2006). The origin of Fe-Ni metals in eucrites and implications for impact history of the HED parent body. *Lunar Planet. Sci. XXXVII*. Lunar Planet. Inst., Houston #1678 (abstr.).

Yamaguchi A., Barrat J-A., Ito M. and Bohn M. (2011) Posteucritic magmatism on Vesta: evidence from the petrology and thermal history of diogenites. *J. Geophys. Res.* **116**, E08009.

Yang J., Goldstein J.I., and Scott E.R.D. (2008) Metallographic cooling rates and origin of IVA iron meteorites. *Geochim. Cosmochim Acta* **72**, 3043-3061.

Yang, J., Goldstein, J.I. and Scott, E.R.D. (2010). Main-group pallasites: Thermal history, relationship to IIIAB irons, and origin. *Geochim. Cosmochim. Acta.* **74**, 4471-4492.

Ziegler K. andYoung E. D. (2007). Pallasite, mesosiderite, and HED $\Delta^{17}O$ signatures: The details. *Lunar Planet. Sci. XXXVIII*. Lunar Planet. Inst., Houston #2021 (abstr.).

Ziegler K. and Young E.D. (2011) Oxygen isotope composition of main-group pallasites. *Lunar Planet. Sci. XLII*. Lunar Planet. Inst., Houston #2414(abstr.).

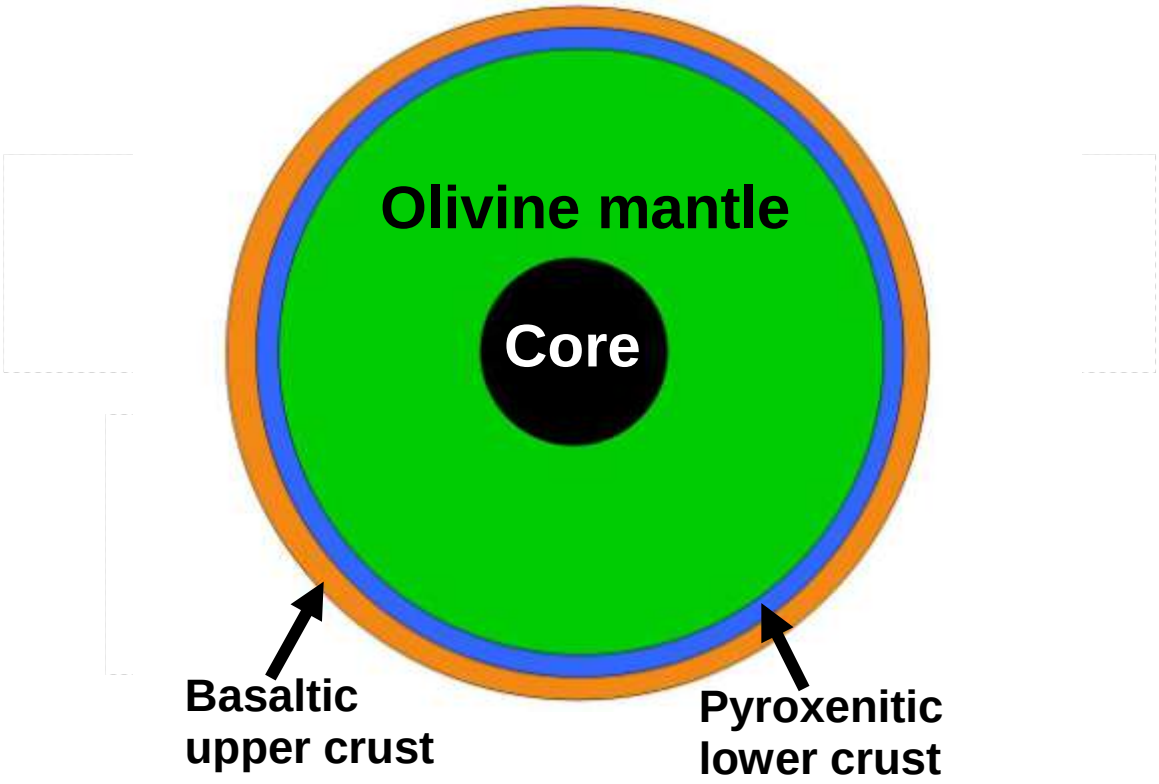

Fig. 1 Schematic cross-section of the interior of a hypothetical differentiated asteroid formed as a result of melting of a chondritic starting composition. The exact thickness of the individual layers calculated by modelling studies (Ruzicka et al., 1997; Righter and Drake, 1997; Mandler and Elkins-Tanton, 2013; Toplis et al., 2013) is dependent on the assumed starting composition.

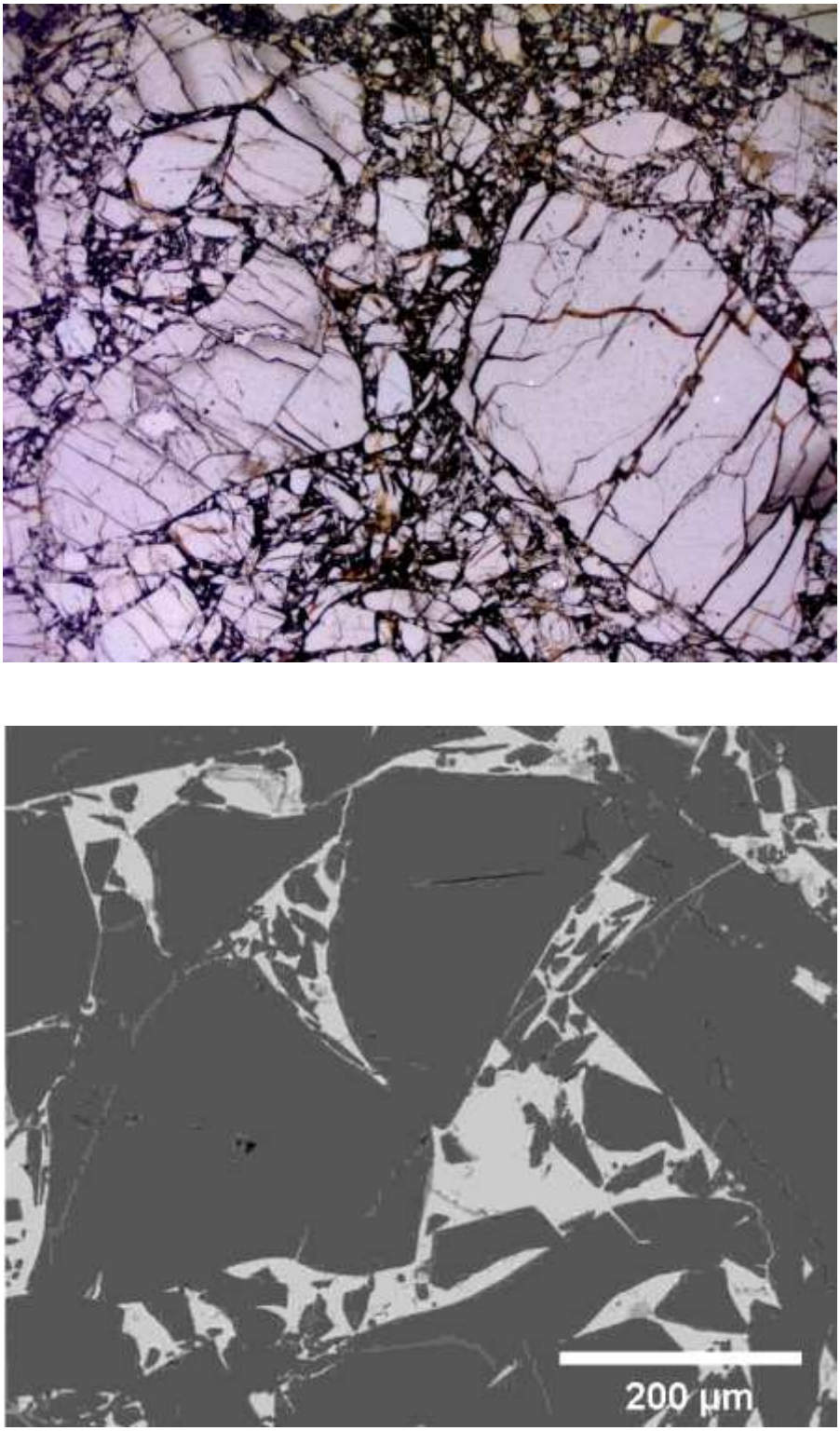

Fig. 2. Vaca Muerta dunite clast. Fig 2a (top). Vaca Muerta olivine-rich clast showing cataclastic textured olivines in a dark matrix. (plane polarized light. Field of view 7mm). Fig 2b (bottom). Backscattered electron image of the Vaca Muerta olivine-rich clast showing that the angular olivine fragments are enclosed in a sulphide-rich matrix.

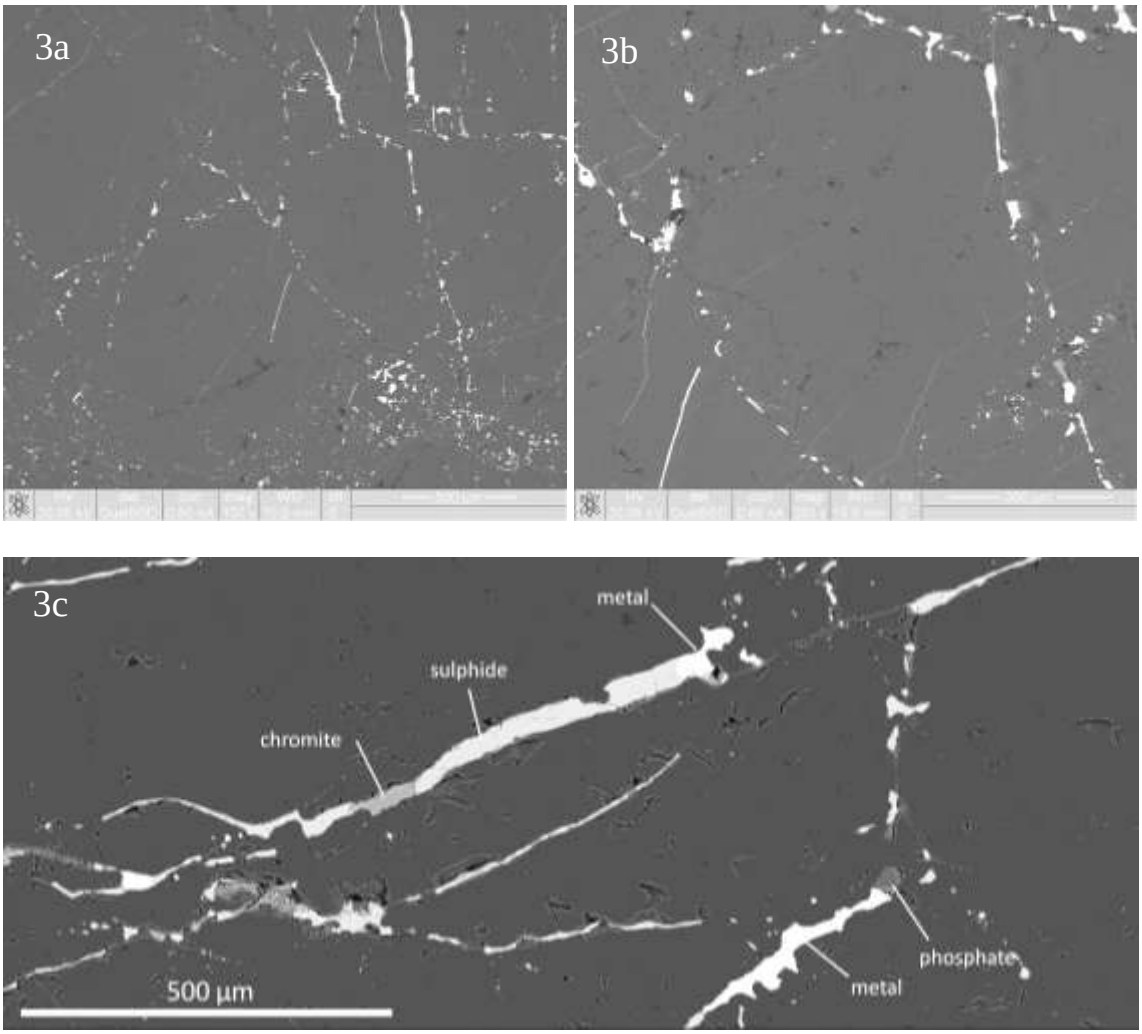

Fig. 3 Backscattered electron images of Mount Padbury inclusion "N". Fig. 3a (left): Large centimetre-sized olivines (McCall 1966) are traversed by a network of thin veinlets mainly composed of iron sulphide with accessory chromite, phosphate and Fe,Ni metal Note that not all fractures are completely occupied by accessory phases. Fig. 3b (right): Higher magnification image of the central area of Fig. 3a showing thin (10 - 30µm) veinlets and blebs of iron sulphide along the margin of angular olivine grains. Fig. 3c (bottom): detail of area in the top central part of Fig. 3a. Olivine is essentially unzoned and traversed by fracture sets filled by sulphide, metal, chromite and phosphates.

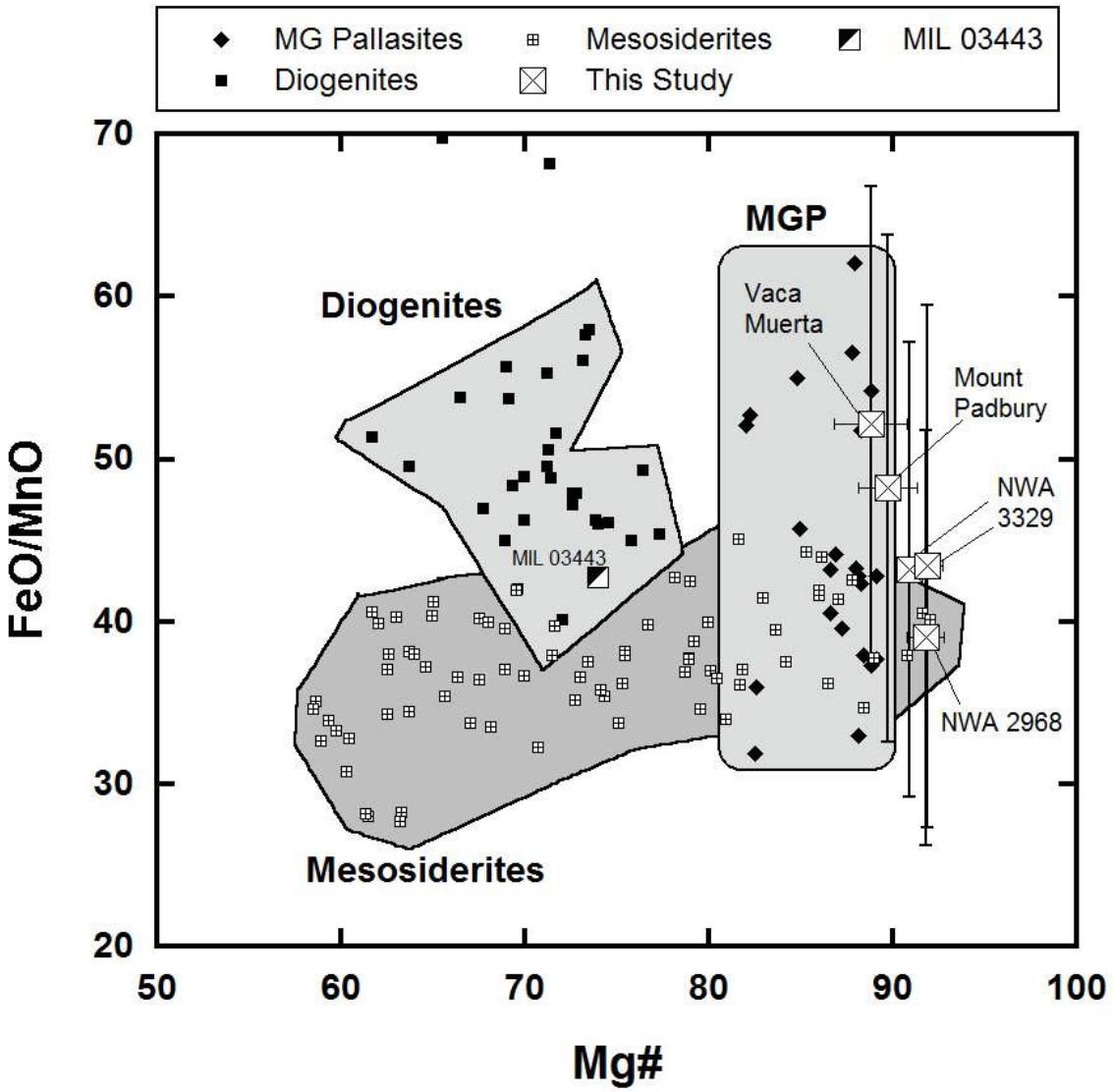

Fig. 4 The composition of olivine from mesosiderite dunites, olivine-rich clasts and related olivine-rich meteorites (NWA 2968, NWA 3329) compared to main-group pallasites, mesosiderites and diogenites. Error bars 2σ. Main Group Pallasite data: Mittlefehldt, 1980; Mittlefehldt et al., 1998; Boesenberg et al., 2012. Diogenite data: Sack et al., 1991; Mittlefehldt et al., 1998; Mittlefehldt, 2000; Irving et al., 2003; Barrat et al., 2006; Beck and McSween, 2010; Shearer et al., 2010. Mesosiderite data: Delaney et al., 1980; Mittlefehldt, 1980; Prinz et al., 1980; Mittlefehldt et al., 1998; Terribilini et al., 2000; Kong et al., 2008 **Note:** olivine in mesosiderites occurs as small grains in the matrix and as coarse cm-sized grains and dunitic clasts. The data of Mittlefehldt (1980) was exclusively from these larger grains. In comparison, the largest dataset plotted is from Delaney et al. (1980) which includes analyses from all mesosiderite olivine types. The large coarse-grained olivines and the smaller matrix types are likely to be from different sources.

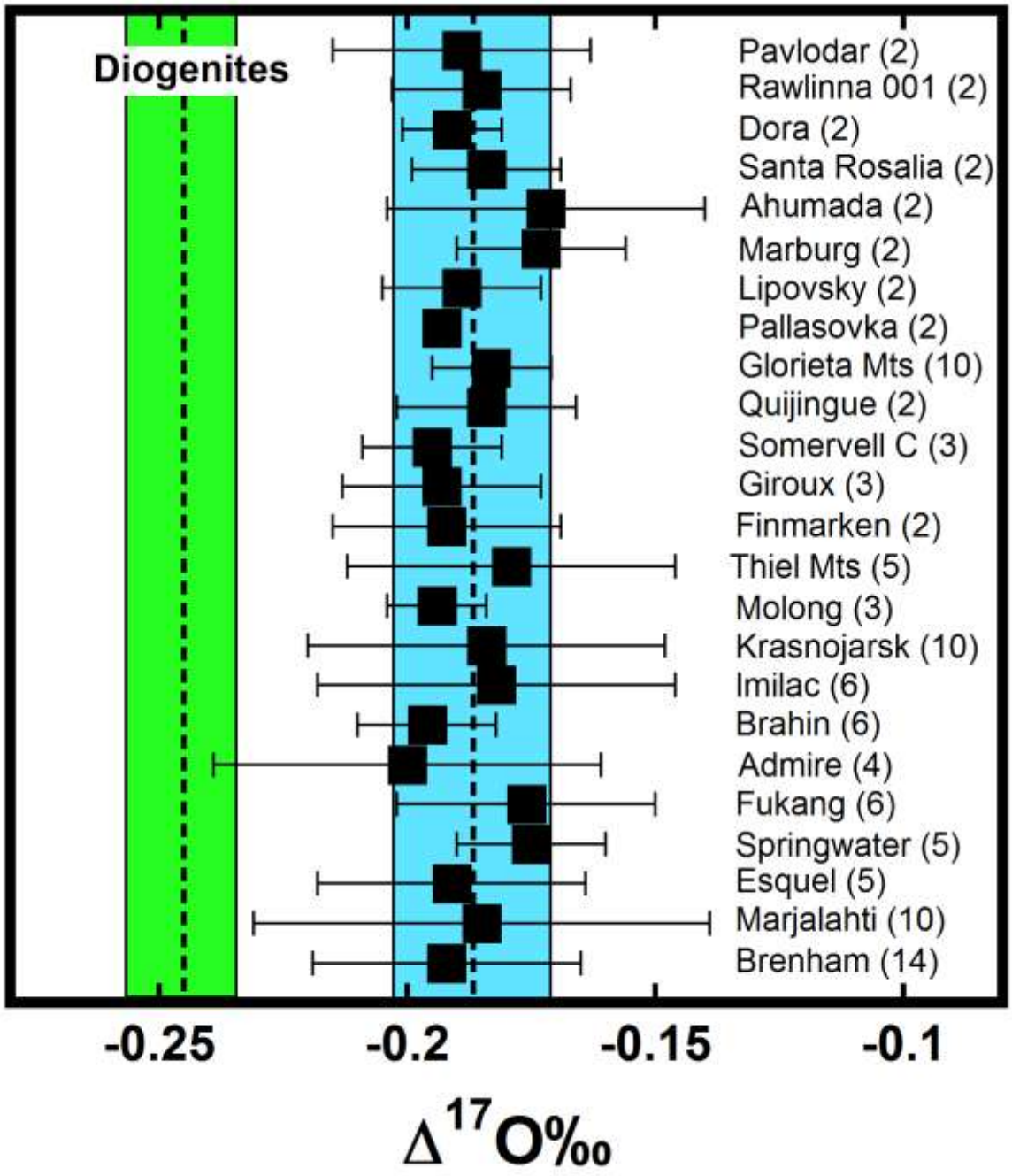

Fig. 5 Oxygen isotope composition of 24 main-group pallasites compared to the diogenite data of Greenwood et al. (2014). Shaded zones represent the ±2σ variation on the group mean $\Delta^{17}O$ values for diogenites and main-group pallasites. Error bars shown for individual pallasite samples represent the ±2σ variation of the analyzed replicates for that sample. Vertical dashed lines represent the mean $\Delta^{17}O$ values for the main-group pallasites (this study) and diogenites (Greenwood et al. 2014).

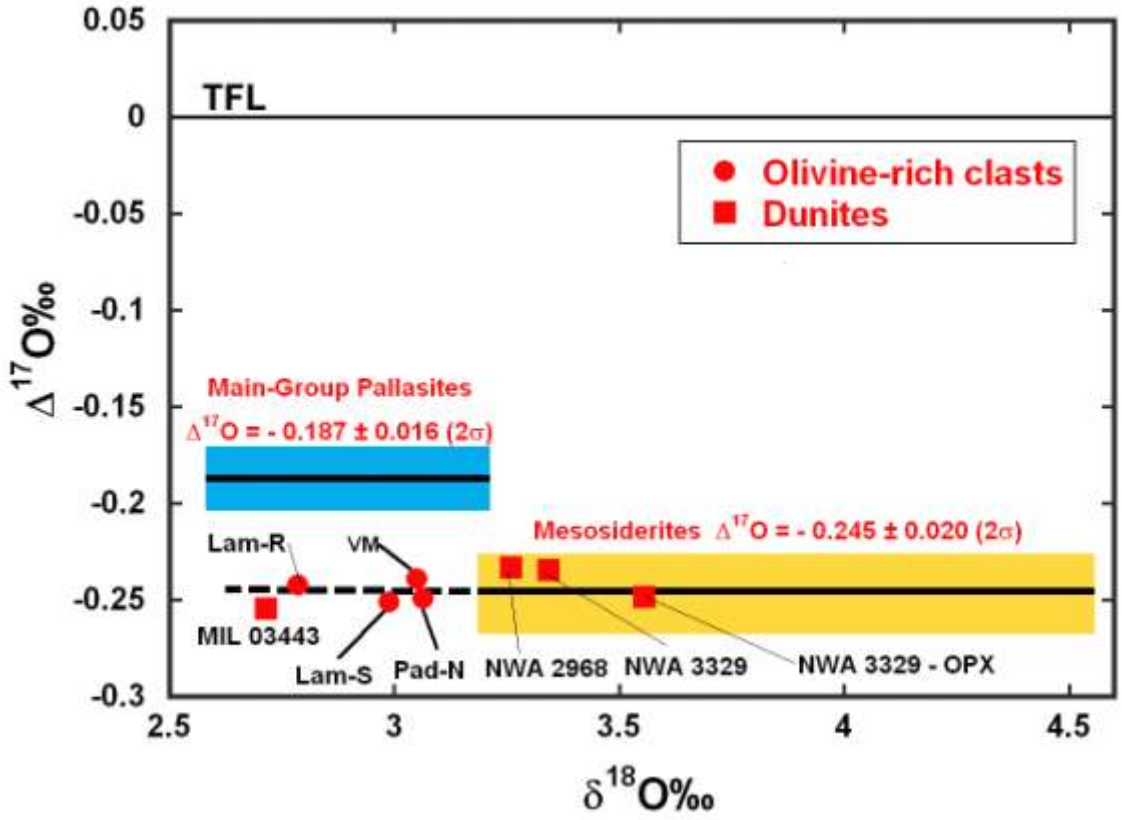

Fig 6. Oxygen isotope composition of olivine-rich clasts in mesosiderites compared to main-group pallasites (this study) and other mesosiderite samples (Greenwood et al., 2006). Shaded zones show the ±2σ variation on group mean values. Lam = Lamont, VM = Vaca Muerta, Pad = Mount Padbury. TFL = terrestrial fractionation line. Analysis of MIL 03443 from Greenwood et al. (2014).

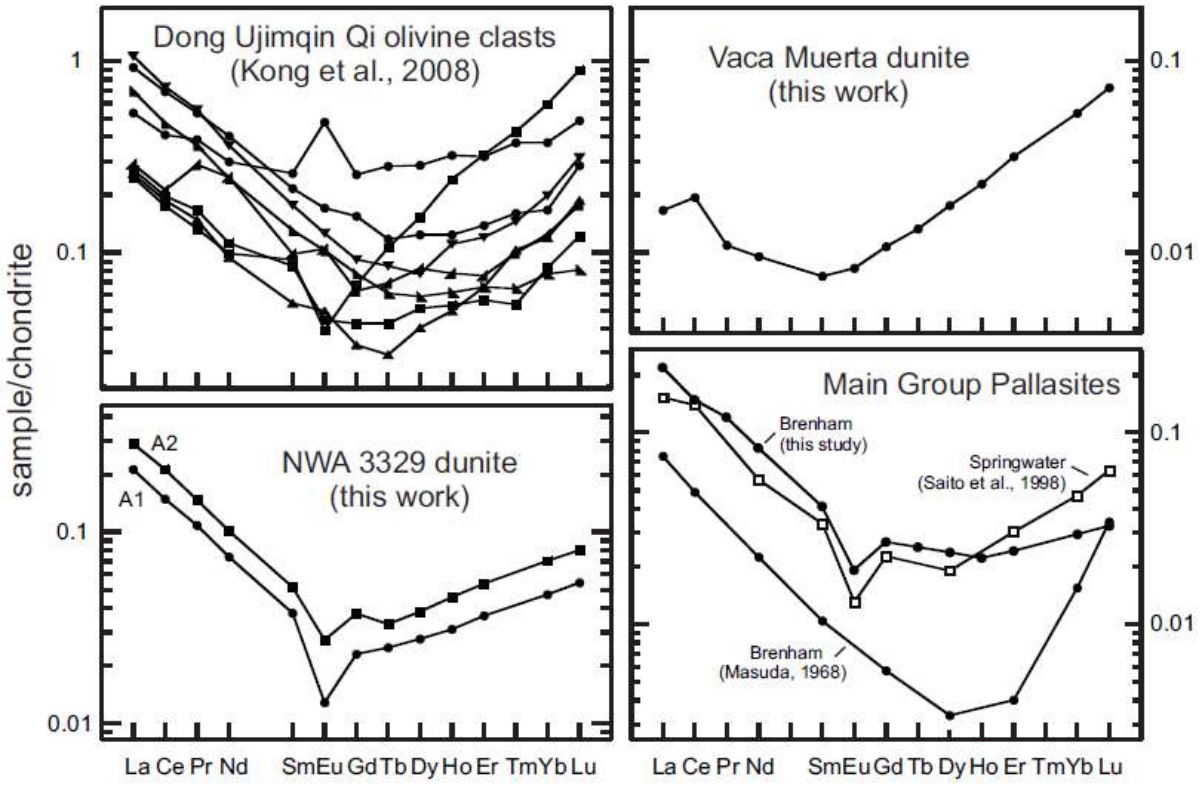

Fig. 7 CI normalized Rare Earth Element plot for the Vaca Muerta and NWA 3329 dunitic clasts compared to that of olivine clasts from the Dong Ujimqin Qi mesosiderite (Kong et al., 2008), and olivine from the Brenham and Springwater pallasites (Masuda, 1968; Saito et al., 1998; this study).

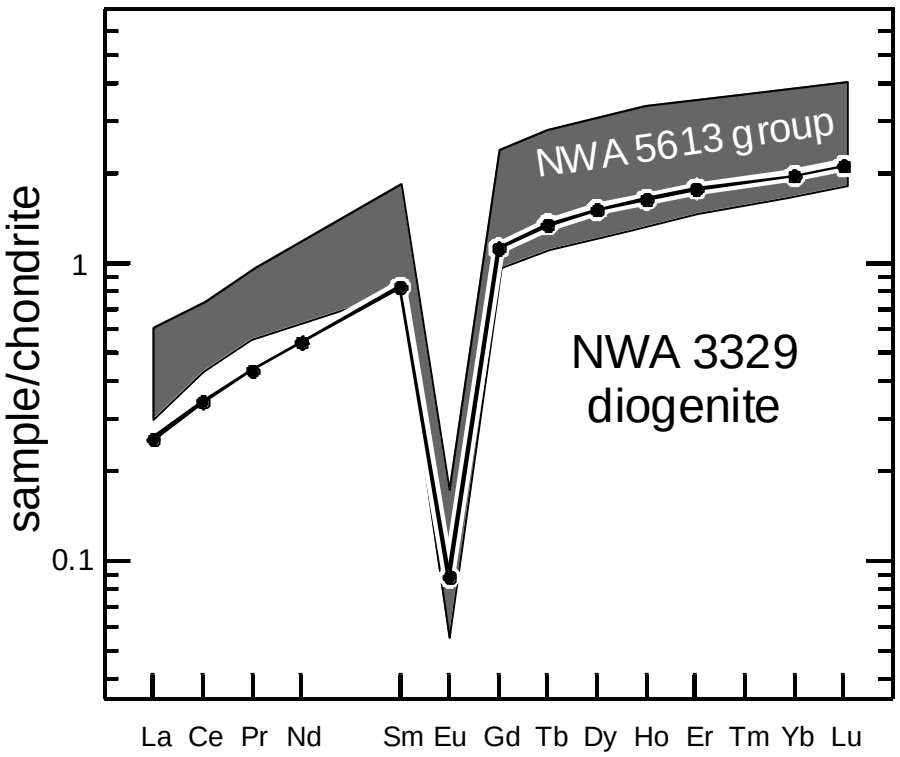

Fig. 8 CI normalized Rare Earth Element plot for the NWA 3329 diogenitic clast compared to some diogenites (NWA 5613 group, Barrat et al. 2010b).

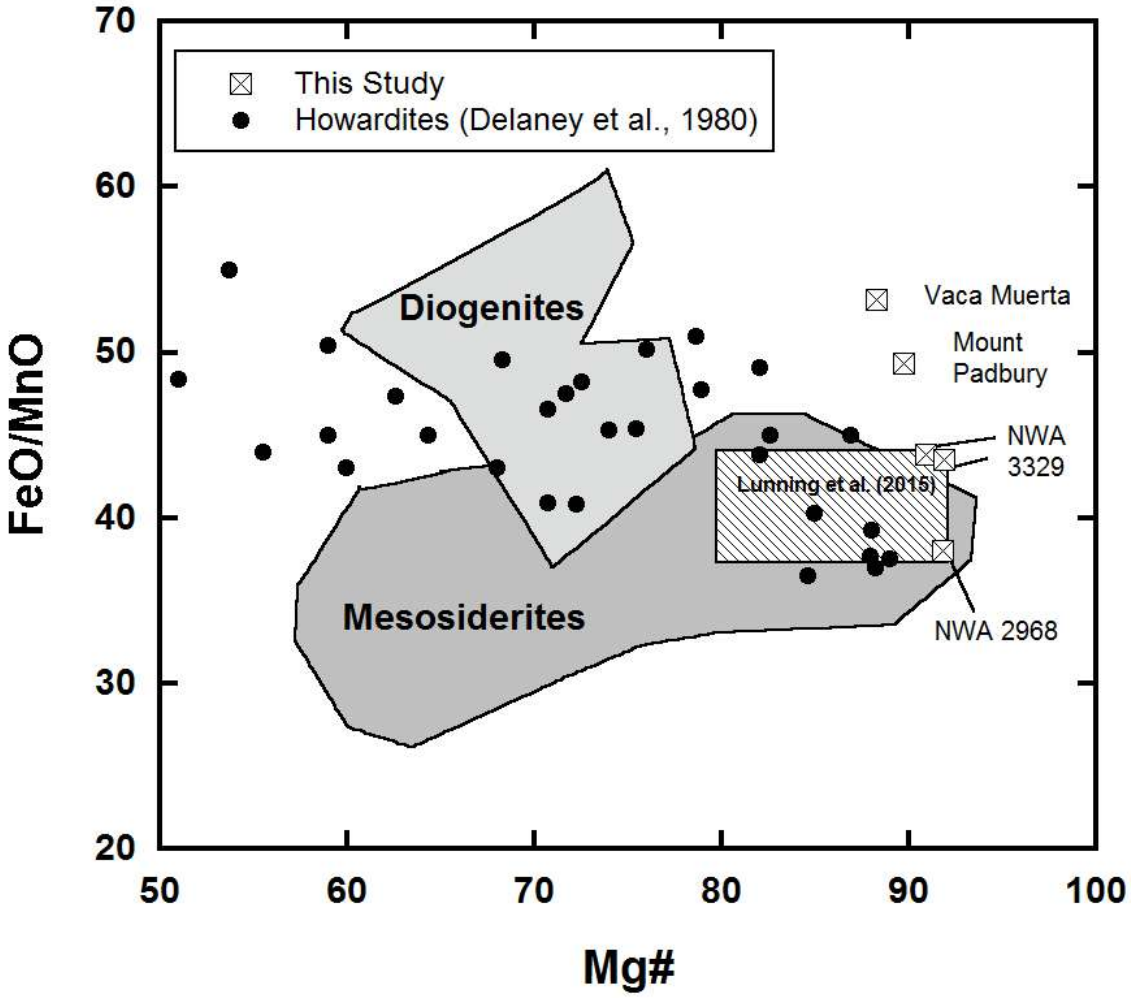

Fig. 9 The composition of olivines in howardites (Delaney et al., 1980; Lunning et al., 2014) shown in relation to mesosiderite olivines (Delaney et al., 1980; this study). Fields for diogenites and mesosiderites are as defined in Fig.4. Diagonal ruled box: howardite olivine data of Lunning et al. (2014).

TABLE 1

	N	$\delta^{17}O$‰	1σ	$\delta^{18}O$‰	1σ	$\Delta^{17}O$‰	1σ
Admire	4	1.362	0.071	2.978	0.162	-0.200	0.020
Ahumada EATG	2	1.377	0.024	2.955	0.077	-0.172	0.016
Brahin	6	1.413	0.141	3.069	0.272	-0.196	0.007
Brenham	14	1.335	0.096	2.913	0.19	-0.192	0.014
Dora EATG	2	1.394	0.011	3.023	0.011	-0.191	0.005
Esquel	5	1.404	0.093	3.043	0.177	-0.191	0.013
Finmarken	2	1.29	0.196	2.826	0.352	-0.192	0.011
Fukang	6	1.333	0.148	2.878	0.296	-0.176	0.013
Giroux	3	1.283	0.178	2.816	0.352	-0.193	0.010
Glorieta Mountains EATG	3	1.356	0.146	2.935	0.27	-0.183	0.006
Imilac	6	1.424	0.097	3.064	0.195	-0.182	0.018
Krasnojarsk	10	1.354	0.118	2.933	0.247	-0.184	0.018
Lipovsky EATG	2	1.273	0.028	2.789	0.037	-0.189	0.008
Marburg EATG	2	1.462	0.009	3.118	0.001	-0.173	0.008
Marjalahti	10	1.379	0.073	2.985	0.148	-0.185	0.023
Molong	3	1.421	0.038	3.08	0.064	-0.194	0.005
Pallasovka EATG	2	1.3	0.055	2.848	0.104	-0.193	0.001
Pavlodar	2	1.401	0.183	3.033	0.325	-0.189	0.013
Quijingue – EATG	2	1.226	0.078	2.69	0.165	-0.184	0.009
Rawlinna 001 EATG	2	1.292	0.022	2.817	0.059	-0.185	0.009
Santa Rosalia EATG	2	1.42	0.006	3.06	0.026	-0.184	0.007
Somervell County	3	1.314	0.123	2.879	0.247	-0.195	0.007
Springwater	5	1.482	0.016	3.161	0.019	-0.175	0.008
Thiel Mountains	5	1.433	0.187	3.075	0.382	-0.179	0.017
AVERAGE VALUES	**103**	**1.364**	**0.065**	**2.957**	**0.12**	**-0.187**	**0.008**
Mesosiderite olivine-rich clasts and related dunites							
Lamont olivine "R" EATG	2	1.218	0.143	2.785	0.278	-0.242	0.003
Lamont olivine "S" EATG	2	1.315	0.130	2.988	0.267	-0.251	0.010
Mount Padbury incl. "N" EATG	3	1.356	0.095	3.063	0.174	-0.249	0.006
NWA 2968 bulk EATG	2	1.476	0.045	3.259	0.082	-0.233	0.002
NWA 3329 - olivine- rich EATG	2	1.518	0.002	3.341	0.016	-0.234	0.006
NWA 3329- OPX-rich EATG	2	1.616	0.029	3.555	0.04	-0.248	0.008
Vaca Muerta dunite clast interior	8	1.360	0.056	3.049	0.111	-0.239	0.010

Table 2. Representative mineral analyses.

		SiO2	TiO2	Al2O3	Cr2O3	FeO	MnO	MgO	CaO	Na2O	K2O	P2O5	NiO	V2O3	Total	mg#	±1σ	FeO/MnO	±1σ
Dunite clast Vaca Muerta																			
olivine	n=183	40.75	0.01	0.01	0.03	10.97	0.21	48.65	0.01	0.01	n.d.	0.01	0.01	-	100.67	88.8	1	52.2	7.3
stanfieldite	n=10	1.04	n.d.	0.01	0.05	3.91	0.51	21.76	25.99	n.d.	n.d.	48.43	0.01	-	101.71	90.8	4.2	7.7	4.8
chromite	n = 1	0.08	0.06	8.72	57.29	26.66	1.18	3.51	n.d.	n.d.	n.d.	n.d.	0.05	-	97.55	19.0		22.6	
Dunite clast Mount Padbury																			
olivine	n=128	41.42	0.01	0.01	0.05	10.12	0.21	49.33	0.03	0.01	n.d.	0.01	0.03	-	101.23	89.7	0.8	48.2	7.8
chromite	n=5	0.09	0.05	7.69	57.41	25.85	1.01	3.78	n.d.	n.d.	n.d.	0.01	0.03	-	95.92	20.7	1.6	25.6	5.5
Dunite NWA 2968																			
olivine	n=66	41.73	< 0.03	< 0.03	0.05	8.17	0.21	51.11	< 0.03	< 0.03	< 0.03	< 0.03	n.d.	n.d.	101.32	91.8	0.5	39.0	6.4
orthopyroxene	n=27	58.41	< 0.03	0.33	0.43	5.26	0.21	35.71	0.93	< 0.03	< 0.03	< 0.03	n.d.	n.d.	101.31	92.4	0.2	26.7	5.6
Dunite NWA 3329, clast A																			
olivine	n=51	41.45	< 0.03	< 0.03	0.04	8.98	0.21	50.47	< 0.03	< 0.03	< 0.03	< 0.03	< 0.03	< 0.03	101.25	90.9	0.2	43.2	7.0
orthopyroxene	n=5	58.17	0.03	0.50	0.50	5.92	0.17	35.18	0.80	< 0.03	< 0.03	< 0.03	0.08	< 0.03	101.34	91.4	0.2	34.3	2.2
chromite	n=4	0.13	< 0.03	2.94	64.36	26.52	0.79	3.79	< 0.03	< 0.03	< 0.03	< 0.03	0.03	0.91	99.40	20.3		33.7	
Dunite NWA 3329, clast B																			
olivine	n=84	41.33	< 0.03	< 0.03	0.03	8.09	0.19	51.38	< 0.03	< 0.03	< 0.03	< 0.03	n.d.	n.d.	101.07	91.9	0.4	43.4	8.1
chromite	n=1	0.05	< 0.03	8.52	60.47	23.84	0.84	6.09	0.04	0.04	< 0.03	< 0.03	0.05	0.61	100.50	31.3		28.3	
chromite	n=1	0.06	< 0.03	12.41	56.01	22.91	0.89	7.16	0.05	0.00	< 0.03	< 0.03	0.06	0.70	100.17	35.8		25.9	
Diogenite NWA 3329																			
orthopyroxene	n=92	53.30	0.09	0.66	0.43	20.12	0.69	22.83	2.13	< 0.03	< 0.03	< 0.03	n.d.	n.d.	100.23	66.9	0.6	29.4	2.2

Table 3. Trace element analyses (ppm).

	VM unleached dunite	NWA3329A1 dunite residue	NWA3329A2 dunite residue	NWA 3329 diogenite residue	Brenham olivine
Li	1.64	0.42	1.75	2.31	0.61
Sc	1.55	0.39	0.86	23.19	0.47
Ti	81	23	41	1029	12
V	21.12	13.52	39.43	129	4.19
Cr	392	1258	2969		117
Co	16.94	142	79.8	10.07	5.3
Ni	369	1872	1005	44.83	14
Cu	5.80	4.47	3.64	0.53	0.05
Zn	1.84	0.42	0.44		3.99
Ga	0.05	0.092	0.21	0.63	0.33
Rb	0.014	0.12	0.22	0.041	0.20
Sr	0.846	0.284	0.253	1.76	0.170
Y	0.0375	0.0495	0.0836	2.60	0.0356
Zr		0.24	0.50	4.29	0.32
Ba	0.64	4.73	3.25	22.71	1.14
La	0.0039	0.0498	0.0677	0.0602	0.0525
Ce	0.0116	0.0889	0.127	0.205	0.0909
Pr	0.00099	0.00983	0.0134	0.0397	0.0112
Nd	0.00443	0.0344	0.0471	0.253	0.0393
Sm	0.00115	0.00576	0.00786	0.127	0.00640
Eu	0.00048	0.00075	0.0016	0.00516	0.0011
Gd	0.002214	0.00476	0.00774	0.232	0.00561
Tb	0.000498	0.000935	0.00124	0.0506	0.000958
Dy	0.00447	0.00703	0.00978	0.385	0.00061
Ho	0.00129	0.00176	0.00259	0.0927	0.00127
Er	0.00527	0.00608	0.00896	0.296	0.00405
Yb	0.00896	0.00791	0.01186	0.331	0.00503
Lu	0.00178	0.00134	0.00198	0.0524	0.00081
Hf		0.00740	0.014	0.144	0.010